PL-TR-93-3053

AD-A274 973

PL-TR-
93-3053 ②

FLOWING DPF DESIGN FOR PROPULSION EXPERIMENTS

G.H. Miley
J.B. Javedani
B.A. Temple
H. Kislev
R.T. Nachtrieb

Fusion Studies Laboratory
Nuclear Engineering Department
University of Illinois
Urbana, Illinois 61801−2984

August 1993

Final Report

DTIC
ELECTE
JAN 13 1994
S E D

94-01439

94 1 12 026

NOTICE

When U.S. Government drawings, specifications, or other data are used for any purpose other than a definitely related Government procurement operation, the fact that the Government may have formulated, furnished, or in any way supplied the said drawings, specifications, or other data, is not to be regarded by implication or otherwise, or in any way licensing the holder or any other person or corporation, or conveying any rights or permission to manufacture, use or sell any patented invention that may be related thereto.

FOREWORD

This final report was submitted by the University of Illinois, Urbana, Illinois under contract F29601-90-K-0048 with the OLAC PL/RKFE Branch, at the Phillips Laboratory, Edwards AFB CA 93524-7680. OLAC PL Project Manager was Dr Frank Mead.

This report has been reviewed and is approved for release and distribution in accordance with the distribution statement on the cover and on the SF Form 298.
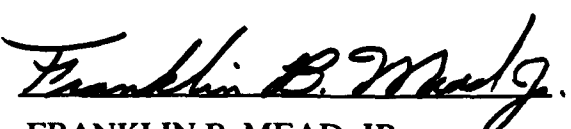
FRANKLIN B. MEAD, JR.
Project Manager
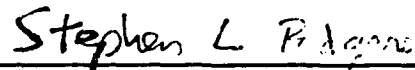
STEPHEN L. RODGERS
Chief, Emerging Technologies Branch

LEONARD C. BROLINE, Lt Col, USAF
Director,
Fundamental Technologies Division
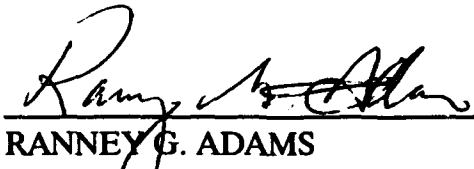
RANNEY G. ADAMS
Public Affairs Director

DTIC QUALITY INSPECTED 5

Accesion For		
NTIS CRA&I		☒
DTIC TAB		☒
Unannounced		☐
Justification		
By		
Distribution /		
Availability Codes		
Dist	Avail and / or Special	
A-1		

REPORT DOCUMENTATION PAGE

1. AGENCY USE ONLY (LEAVE BLANK)	2. REPORT DATE August 1993	3. REPORT TYPE AND DATES COVERED Final Report 3 May 90 – 30 Aug 92

4. TITLE AND SUBTITLE

FLOWING DPF DESIGN FOR PROPULSION EXPERIMENTS

6. AUTHOR(S)

G.H. Miley; J.B. Javedani; B.A. Temple; H. Kislev; R.T. Nachtrieb

5. FUNDING NUMBERS

C: F29601-90-K-0048

PE: 62302F

PR: 3058

TA: 0096

7. PERFORMING ORGANIZATION NAME(S) AND ADDRESS(ES)

Fusion Studies Laboratory
Nuclear Engineering Department
University of Illinois
Urbana, IL 61801-2984

8. PERFORMING ORGANIZATION REPORT NUMBER

9. SPONSORING/MONITORING AGENCY NAME(S) AND ADDRESS(ES)

Phillips Laboratory
Propulsion Directorate
Air Force Materiel Command
Edwards AFB CA 93524-7001

10. SPONSORING/MONITORING AGENCY REPORT NUMBER

PL-TR-93-3053

11. SUPPLEMENTARY NOTES

COSATI CODES: 18/01; 20/08; 20/09

12a. DISTRIBUTION/AVAILABILITY STATEMENT

Approved for Public Release; Distribution Unlimited

12b. DISTRIBUTION CODE

A

13. ABSTRACT (MAXIMUM 200 WORDS)

Recent studies show the Dense Plasma Focus (DPF) to be a viable candidate for use as a long–range space propulsion system with a high power–to–weight ratio. This Air Force contract provided support for study and modification of the University of Illinois (UI) DPF to develop a basic thrust experiment. A key aspect of such a system is to employ gas injection into the DPF electrode region, as opposed to the static fill technique commonly employed in present experimental devices. This report describes the design and initial operation of a prototype gas–puff injection facility, reviews preliminary results, and details plans for future use. The projected performance of a future propulsion system using this technique is also examined. A list of the publications and conference presentations based on research done under this contract is included.

14. SUBJECT TERMS

Dense Plasma Focus (DPF); Fusion Propulsion; MPD Thrusters

15. NUMBER OF PAGES

16. PRICE CODE

17. SECURITY CLASSIFICATION OF REPORT Unclassified	18. SECURITY CLASSIFICATION OF THIS PAGE Unclassified	19. SECURITY CLASSIFICATION OF ABSTRACT Unclassified	20. LIMITATION OF ABSTRACT SAR

NSN 7540-010280-5500

Abstract

Recent studies show the Dense Plasma Focus (DPF) to be a viable candidate for use as a long-range space propulsion system with a high power-to-weight ratio. This Air Force contract provided support for study and modification of the University of Illinois (UI) DPF to develop a basic thrust experiment. A key aspect of such a system is to employ gas injection into the DPF electrode region, as opposed to the static fill technique commonly employed in present experimental devices. This report describes the design and initial operation of a prototype gas-puff injection facility, reviews preliminary results, and details plans for future use. The projected performance of a future propulsion system using this technique is also examined. A list of the publications and conference presentations based on research done under this contract is included.

Acknowledgment

Contents

List of Figures

List of Tables

Summary

Recent studies show the Dense Plasma Focus (DPF) to be a viable candidate for use as a long-range space propulsion system with high power-to-weight ratio[1]. The DPF has a high specific impulse from the fast rundown of the arc and can generate additional energy from fusion produced by the compressed ("pinched") plasma. This contract supported work to modify the University of Illinois (UI) DPF to carry out preliminary experiments aimed at establishing the scaling of the thrust versus the input energy for use as a space propulsion device.

The UI DPF (Mather-type) employed in this study consists of a set of twenty, 2 μf capacitors in parallel (40 μf total capacitance) arranged in four perpendicular arms[2]. The four arms intersect and support the vacuum chamber. Four Trigatron spark gaps, coupled to a 5 ns rise time Marx generator, trigger the four sets of capacitors to discharge simultaneously. The maximum focus current reaches $3\text{-}5 \times 10^5$ Amp. The pinch lasts approximately 40 ns, during which time the plasma temperature and densities reach 1 keV and 10^{19} cm^{-3} respectively.

The original objectives for this work were:

- modify the UI DPF vacuum system, electrodes, and gas inlet system to develop a thrust-producing configuration,

- identify diagnostic methods to measure the thrust levels for such a system,

- study the effects on thrust of varying the following parameters: length and shape of inner electrode, axial magnetic field, background gas pressure, propellant mass flow rate, arc voltage and current,

- conduct a preliminary study to obtain scaling of thrust versus input energy.

During the course of the contract, some changes in the objectives were made, partly because of a lengthy shutdown of the UI DPF due to a non-contract problem. Still, most of the original project objectives were achieved, including successful operation of a new gas puff valve for pulsed injection into the DPF. Specifically, the following tasks were completed:

- design and construction of gas-puff injection system,

- design and construction of a timing circuit to coordinate discharge of capacitors and release of gas into the chamber,

- design of new center electrode and insulator for gas injection system,

- study of center electrode shape and effects on impedance-matching with capacitor bank,

- preliminary study of scaling law of thrust vs. input energy,

1

- identification of a diagnostic suitable for measuring small forces in a high-electromagnetic (EM) noise environment.

This report describes the design and operation of the gas-puff injection facility, recapitulates the results to date and the plans for future use. Publications and presentations based on work done for this contract are also listed.

The University of Illinois DPF Experiment

The UI DPF facility consists of a set of twenty, 2–µf capacitors in parallel (40 µf total capacitance) arranged in four perpendicular arms. The vacuum chamber is located at the intersection of the arms. The four sets of capacitors are discharged simultaneously by triggering four Trigatron spark gaps coupled to a 5 ns rise time Marx generator. An schematic of the electrical system is shown in Figure 1. The peak current during peak is $\sim 3\text{-}5 \times 10^5$ Amp and the pinch lasts approximately 40 ns. Peak temperatures of ~ 1 keV and
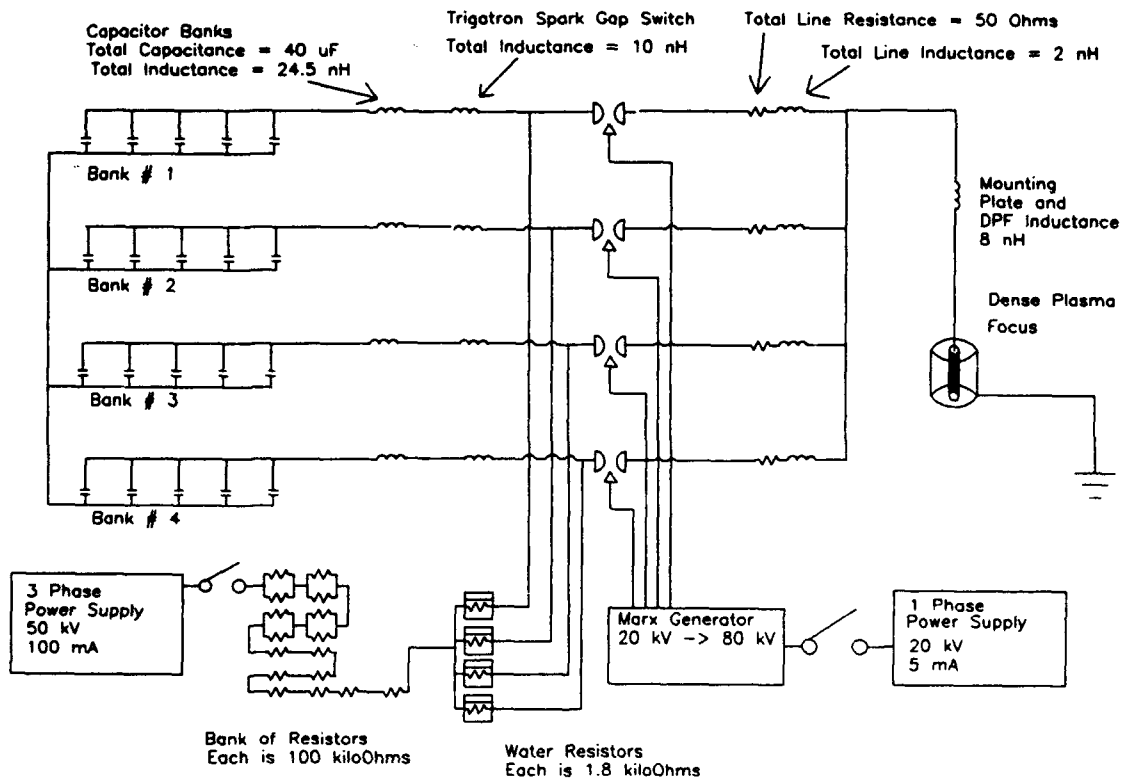
Figure 1. Electrical Schematic of UI DPF System.

CAPACITOR BANK

PLEXIGLASS

MYLAR INSULATING SHEET

SWITCH

CERAMIC INSULATOR

CURRENT SHEET

SPOKE STRUCTURE (PFW)
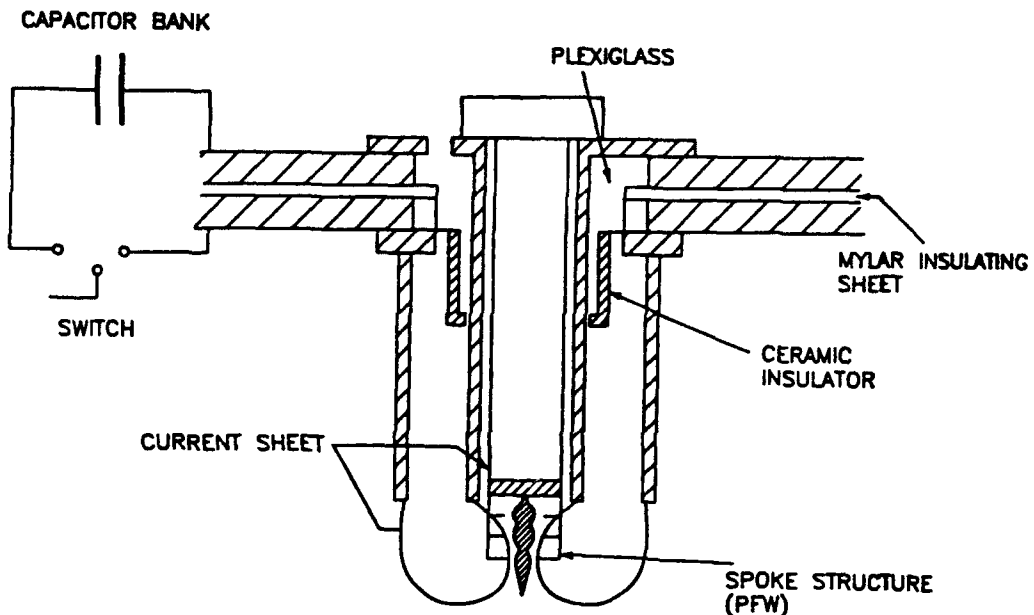
Figure 2. UI Dense Plasma Focus in the Mather Configuration.

densities of $\sim 10^{19}$ cm^{-3} have been measured during the pinch. (See Appendix A for a pictorial tour of the UI DPF facility.)

The UI Mather-type DPF was modified under the present contract to carry out experiments using a novel gas-injection system to simulate DPF operation for propulsion in outer space. This device involves use of a fast operating gas puff valve as described later. A diagram of the UI Mather-type DPF is shown in Figure 2.

Normally the UI DPF operates in a pressurized chamber such that the electrical rundown pinches a portion of the background gas in the chamber between the electrodes. Such operation is common for DPF operation and is denoted as a static-fill operation. In contrast, for space operation, the electrodes would normally be under hard vacuum conditions. To simulate the space environment, the DPF chamber is held at hard vacuum (~60 mTorr) and then a puff of gas is introduced at the breach, and "run down" the electrode by a timed electrical pulse from the capacitor bank.

Gas Injection System

As described in the previous section, development of a gas injection system is a key element in the development of a DPF thruster of the type envisioned. Although

3

several prior designs have injected gases (D_2 and H_2) at the end of the middle of the DPF electrode, none were capable of operating with a coil placed in the middle of the inner electrode for the purpose of pinch stabilization[3]. The coil, which generates an axial magnetic field, is important for a more uniform thrust in repetitive pulsing of the device. While the present configuration does not use a center coil for this initial testing, the device is designed to be able to accommodate one inside the center electrode. Furthermore, this gas injection system would also maintain the same electrode diameter and length for rundown. The present device differs in this respect, from the Coaxial Gas Gun at the Air Force Weapons Lab.[4][5] In this design operational comparisons could readily be made between the gas puff injection system and the static fill method. These earlier designs have been carefully considered in the development of the system described here. However, since this is a "first of the kind" unit, we have spent considerable effort in its design and in experimentally optimizing its performance.

While the present experimental system is designed for operation on D_2 and H_2, a future DPF thruster is envisioned to use D_2 and $^3He_2$ for the fusion fuel while H2 would be added as the propellant. Fortuantely, the D_2 and H_2 experiment provides a good simulation for such future devices.

An illustration of the gas injection system constructed for use with the 10 kJ DPF is shown in Figure 3. It consists of a plenum, approximately 6 in. in diameter and 0.75 in deep, located above the upper conducting plate which is connected to a cylindrical inlet port between the electrodes. The center assembly is 4.5 in. high from the base of the plenum to the end of the ceramic insulator and weighs approximately 20 lbs. The gas flows into the plenum from four gas tubes on the top of the system which branch from a single gas tube coming from a pressurized (~50 Torr) gas cylinder. Gas flows out of the plenum from the inlet port into the vacuum chamber. Gas is confined in the plenum by a gas valve at the intersection of the four tubes at the top of the system and by a ring valve located between the plenum and the inlet port. The ring valve is opened by four solenoids located above the plenum and is attached to the ring by four rods. Additional pieces are used to compress and seal the system against gas leaks. The entire assembly is azimuthally symmetric around the electrodes.

Azimuthal symmetry is a key design goal in this gas injection system. It is essential to ensure an azimuthally uniform radial current flow and gas flow. The plenum, ring valve, and inlet port are constructed so that an azimuthally uniform slug of gas flows between the electrodes when the ring valve is opened. The ring valve opens evenly due to the symmetrical placement of the lifting rods around the ring. The gas tubes are also evenly spaced so that plenum fills with gas in an uniform manner. The gas of the inner electrode, may cause some blockage of the current flow. However, by having the current interruptions evenly spaced around the electrode, the azimuthal symmetry of the current flow is preserved.

All components of the gas injection system are designed to be assembled vertically. This is important due to the vertical orientation of the electrodes for the DPF.

4

SOLENOID
SOLENOID BRACKET
PIECE #10   LIFT ROD PLATE   PIECE #13
PIECE #5   PIECE #9   PIECE #8
PIECE #11
PIECE #7
PIECE #12
PIECE #4   PIECE #1   PIECE #2
PIECE #3
UPPER TRANSMISSION PLATE
LOWER TRANSMISSION PLATE
CERAMIC INSULATOR
OUTER ELECTRODE
PIECE #6
AXIAL MAGNETIC FIELD COIL
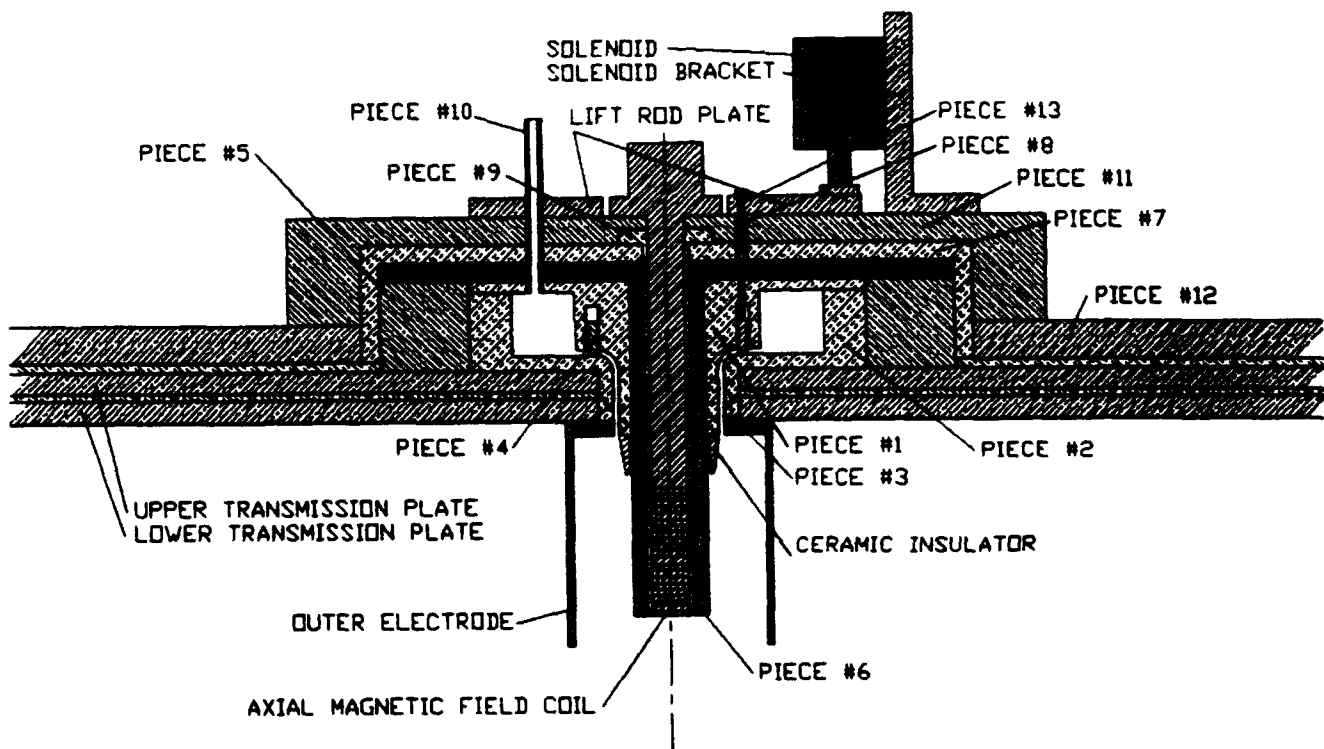
Piece Number	Item Description
1	Valve containment ring
2	Plenum chamber ring
3	Transmission plate seal
4	Valve ring
5	Aluminum conducting ring
6	Inner electrode
7	Electrode containment piece
8	Lift rod guide tube
9	Axial B-field insulating piece
10	Gas extension tube
11	Aluminum cover plate
12	Aluminum compression plate
13	Lift rod

Figure 3. Gas-Injected Plasma Focus, Developed at the University of Illinois.

Only a small area inside the diameter of the top compression plate must be assembled and disassembled in order to install and service the gas injection system. The vertical assembly requires no special tools or great manual dexterity to assemble. The symmetric design of the system allows the pieces to be layered on top of each other without concern for their azimuthal orientation. Thus as long as the proper sequence of assembly is used, assembly and maintenance of the gas injection system can be performed by one person in a short time. This is a significant advantage, since the puff valve is frequently removed for other experiments and then reinserted.

Description of the Gas Puff Valve and Associated Parts.

The discussion of the individual components of the gas valve unit begins with the bottom components system and progresses sequentially to the components at the top. Each part described is numbered and identified in Figure 3.

At the base of the electrodes, the valve containment ring (#1), plenum chamber ring (#2), and transmission plate seal (#3), fit together to form the inlet port. The inlet port forms a cylindrical slit 0.48 cm wide which directs the gas from the base of the plenum to the base of the electrodes. A variety of criteria were considered in the design of the inlet port; its width had to be large enough to guide sufficient amounts of gas to the chamber, but not so large as to inhibit arc formation at the base of the electrodes. Keeping the width of the inlet port small compared to the height of the plenum helps to "squeeze out" any uneven distribution of the gas in the plenum which originates when gas flows out of the gas tubes and into the plenum as the plenum empties into the vacuum chamber. However, if the width is too small, the only way to achieve adequate flow rates is to increase the injection pressure at the base of the electrodes, which can cause instabilities in the arc rundown. Various injection systems used for MPD thrusters utilized inlet ports 0.32 cm or larger at the base of the electrodes. Similar sizes have also been used for coaxial plasma guns (CPGs). Since the operating voltage of the UI DPF is considerably higher than the voltages used on the MPD thrusters or the CPGs, an inlet port width of 0.48 cm is not so large that it inhibits arc formation from the insulator to the anode. Still, it is large enough to allow sufficiently large amounts of gas at moderate pressures to pass from the plenum to the vacuum chamber.

Coupled with the criteria for the inlet port is the criteria for the design of the breech region. The breech region is the area inside the center electrode hole of the upper and lower conducting plates. This is where the gas from the inlet port flows into the vacuum at the base of the inner electrode. The criteria for the breech region covers three areas of concern: radial dimension restrictions, electrical insulation, and vacuum containment.

To avoid widening the diameter of the center electrode hole in the upper and lower conducting plates, it was necessary to fit the inlet port into the existing radial dimension of the conducting plate electrode hole. The width of each piece also had to be limited in order to fit the inlet port between the pieces. The internal radius of the valve

6

containment ring is 2.54 cm, as determined by the radius of the inner electrode. Since the ring will hold the ceramic insulator, it is desirable to keep its width at least 0.95 cm wide, so that the insulator can be machined with a tapered design. The width of the ring in the breech should match the width of the ceramic insulator to ensure a smooth gas flow along the insulator surface. If the inlet port is 0.48 cm wide, the plenum chamber ring and the transmission plate seal must be 1.27 cm wide to fit inside the center electrode hole.

A vacuum seal must be maintained on the upper and lower conducting plates by the plenum chamber ring and the transmission plate seal. A good vacuum seal in the breech maintains vacuum in the chamber and stops the leakage of gas past the conducting plates; this prevents arcing between the plates. The presence of the inlet port increases the chances of arcing between the plates due to the increased exposure to gas. Gas leakage along the mylar sheets, which lie between the two plates as an insulator, also represents a potential problem. Thus, in order to isolate the mylar sheets from the gas flow, the original radius of the mylar sheets was decreased by 0.48 cm so the plenum chamber ring could overlap the transmission plate seal and seal along the transmission plate seal's O-ring. Thus overlapping of the two-part piece also gives a smooth path for the gas flow through the inlet port.

Joining the plenum chamber ring and plate seal into one piece in order to completely seal off the plates was ruled out, even though it would give a better vacuum seal. To do alternative experiments with the focus, it is necessary to place the original parts back into the system. Joining the plenum chamber ring and plate seal into one piece would require disassembly of the vacuum chamber under the conducting plates in order to reinstall the original system. Keeping the pieces separate allows replacement of the original parts from the top of the focus. Also, the use of separate pieces make it possible to assemble the system from the top of the chamber. Therefore, installation and changing systems is kept to a one-person job which can be performed quickly.

The inlet port is sealed off from the plenum by the ring valve assembly. The ring valve assembly (#4) is composed of a hollow aluminum disc which rides in a slot machined into the upper part of the valve containment ring. The inlet port is sealed by compression on an O-ring at the base of the chamber ring by the valve containment ring. The downward force required is exerted by four springs evenly spaced around the ring valve, which is sealed by two O-rings on each side. A pair of O-rings are used on each side of the value ring in order to keep it as vertical as possible as it moves up and down in the valve slot. The O-rings used at the base of the chamber ring and on the sides of the ring are Viton O-rings. Viton O-rings require very little vacuum grease to seal along a surface. This is desirable to avoid possible contamination of the ceramic insulator by vacuum grease that might be carried down through the inlet port by the gas flow. The lift rod guide tube, cemented to the valve containment ring, guides the lifting rods (#13) through the containment plates and the inner electrode. The sleeve has additional O-rings around the lifting rods to ensure a vacuum seal and insulate the ring from the inner electrode so any gas which may leak past the ring will not arc from the inner electrode

7

through the inlet port to the outer electrode. The lifting rods are attached to the lift rod plate which is attached to four evenly spaced solenoids. The lift rod plate is needed to attach the lift rods to the solenoids, since the solenoids will not fit directly above the lift rods.

The spring and solenoid sizes on the ring valve assembly had to be experimentally determined. The amount of wall friction exerted by properly sealing O-rings on the ring could not be calculated. Thus the spring force needed to compress the O-ring at the base of the plenum chamber ring was found by testing different sizes of springs in the ring valve. Once the spring size was determined, the solenoid strength could be found. Original plans had the solenoids placed under the aluminum containment piece. However, initial tests with smaller solenoids did not successfully lift the ring up against the force of the springs. Larger solenoids were used to achieve a quick opening ring. With the use of these large solenoids, it was then necessary to move the solenoid outside the aluminum containment piece.

A plenum was placed between the gas lines and the inlet port to allow the gas to reach equilibrium before opening the ring valve. The plenum is sealed off from the inlet port by compression of an O-ring by the ring valve at the base of the plenum. Uniformly lifting the ring valve off the O-ring and opening the inlet port gap gives a consistent slug flow of gas into the inlet port from the plenum. The amount of gas injected into the chamber depends upon the size of the plenum and the gas pressure in the plenum as described later in the section "Puff Valve". The radial thickness of the plenum is limited by the diameter of the compression plate and the radial thickness of the aluminum conducting ring. The existence of the plenum alters the path of the current flow from the conducting plate to the inner electrode. The current must flow an additional distance proportional to the height and width of the plenum. This additional distance increases the resistance and lowers the efficiency of the system. Thus, the plenum height was limited to 1.91 cm, in order to minimize the increase in resistance. The resulting volume of the plenum is approximately 367 cm^3. Since the plenum size was fixed, the amount of gas must be varied by changing the pressure in the plenum. Additional gas can be added to the flow by leaving the gas valve on the incoming gas line open. Thus, all gas from the gas lines and the gas cylinder will drain into the plenum when the ring valve is open.

The gas lines are connected to the plenum by a gas extension tube (#10). The extension tube is glued onto the containment ring with PVC cement. These tubes insulate the gas flow from the inner electrode. This is necessary so arcing cannot occur from the inner electrode through the plenum and inlet port to the outer electrode. Arcing is also possible from the inner electrode to the aluminum cover plate (#11) if the gas is not isolated from the current flow. The gas extension tube is symmetrically located between the lifting rods.

Next to the plenum is the aluminum conducting ring (#5), which allows current flow from the upper conducting plate to reach the inner electrode. The height of the aluminum ring is the same as the valve containment ring and the plenum chamber ring to

8

allow for compression of the O-rings of the plenum pieces. The radius of the aluminum conducting ring was made as large as possible, in order to maximize the conducting surface area between the upper conducting plate and the inner electrode. The conducting surface area with the redesigned inner electrode is 217.87 cm^2 larger than the original contact surface area.

Lying on top of the plenum and the aluminum conducting ring is the inner electrode (#6). The radius of the base plate of the inner electrode was enlarged to 11.89 cm, the same dimension as the outer radius of the aluminum conducting plate. An extension of the base plate was necessary to maximize the conducting surface area between the electrode and the conducting ring. To maintain the same electrode length exposed beyond the ceramic insulator, the length of the inner electrode was extended by 0.90 cm to compensate for the height of the plenum. The inner and outer radii of the inner electrode shaft are unmodified from the original dimensions of 1.59 cm and 2.54 cm respectively.

The aluminum cover plate (#7) lies over the inner electrode to seal the vacuum around the aluminum conducting piece and the gas injection components. The bottom of the cover plate lies on top of a rubber gasket which seals the aluminum conducting ring from the aluminum compression plate. O-rings exist on both faces of the cover plate to seal any vacuum leaks or gas leaks from the lift rod guide tube (#8) and the gas connecting tubes. The height of the cover plate is made so that all O-rings can be compressed to hold vacuum.

Vacuum inside the inner electrode is maintained by the axial B-field insulating piece (#9) which fits around the solenoid coil used to generate the axial magnetic field in the pinch region and extends to the bottom of the inner electrode. The axial B-field insulating piece also separates the vacuum region from the solenoid and seals the vacuum with O-rings located at the top flange of the piece.

Compression on the cover plate and the axial B-field insulating piece is exerted by the aluminum cover plate, which maintains its downward force on the components by twelve bolts which screw into the aluminum pressure plate (#12). The aluminum cover plate has holes evenly placed around it through which the lift rod guide tubes and the gas connecting tubes are fitted. Mounting brackets are placed on top of the aluminum cover plate to secure the solenoids used to lift the ring valve.

Retention of the axial magnetic field coil for the gas-injected experiment represented a further restriction on the valve design. The manufacturer of the valve containment ring requires precise machining of the ring valve in order to achieve gas containment and vacuum seal. Considerable fine adjustments were performed on the ring in order to achieve a vacuum seal. Constant opening of the valve requires periodic adjustment of the O-rings on the ring valve.

The timing circuit is also utilized to minimize the leakage. After pressurizing the plenum, the opening time of the ring is set to be sufficiently short to prevent significant

leakage. Since the plenum can be quickly pressurized to the desired pressure, maintaining plenum pressure is not a problem. The timing circuit opens the gas valve to the plenum at a given time to pressurize the plenum and then opens the ring valve after a short delay. Achieving the correct time intervals for the operation of the ring valve is tedious but important to successful operation of this system. Further discussion of operation and testing of both the timing circuit and the gas valve is given later in Section "Insulator."

Inner Electrode Design.

In order to effectively use the gas puff system, the inner electrode on the DPF was redesigned. Electrode geometries with different impedances affect rundown characteristics. The power delivery system and the load behave like connected transmission lines: if the impedance are properly matched, the system behaves as an underdamped or overdamped RLC circuit. The system and load impedances must match to obtain total voltage transmission from the power delivery system to the load. If the reactance of the system and the added load do not equal zero, the current and the voltage do not have the same phase. For total voltage transmission, the sum of the reactance of the system and the load must be zero.

The inductance of the electrodes increases with the ratio of the inner and outer electrodes radii. However, a desired gas density between the electrodes requires an adequate volume between the electrodes. Thus electrode inductance couples with the gas density introduced by the gas puff between the electrodes.

An electrode design for obtaining the highest axial velocity should have a small inductance and the smallest possible radius.

To examine these issues, 15 basic designs were examined through a modified DPF circuit-equivalent code, based on tapering the radius and chamfering the end of the electrodes, which was included explicitly in the code. Graphs of inductance versus axial length and axial velocity were plotted versus time for all 15 designs. Appendix B presents these designs and graphs. Appendix C presents the Fortran code used to evaluate the designs.

Gradually tapered designs increased the inductance by nearly an order of magnitude compared to the straight electrode. Designs with a sharp curvature in the electrode had nearly the same inductance as the unmodified (straight) electrode. The straight designs gave the highest axial velocities with the lowest inductance values. A sharp curvature at the end of the electrode kept the inductance low, obtaining a large current as the arc neared the end of the electrode.

Figure 4 shows the design (#41) that was finally selected as the best of those evaluated. This electrode was then machined and inserted into the gas flow of the UI Mather-type DPF.

10

22.23 cm

1.11 cm

23.76 cm

5.08 cm
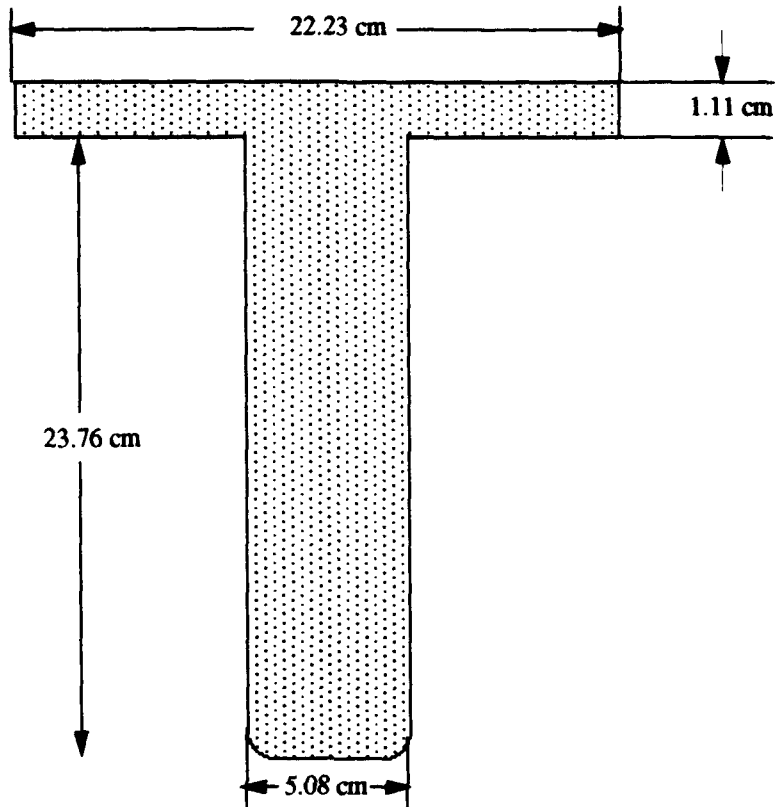
Figure 4. Optimum Center Electrode Design for High Axial Velocity and Low Inductance.

Insulator.

The compression efficiency of the focus rundown depends strongly on proper initiation of the arc along the cathode insulator at the breach. Due to the design changes ma· ·for gas puff injection, it was necessary to redesign the cathode insulator for the UI DPF. The new insulator shown in Figure 5 is constructed of the same type of Lavite ceramic used in the original UI DPF insulator. This selection was based on the observation that ceramic insulators in the arc initiation region increase the rundown and compression effic· ·cy.[2][6] Ceramics apparently provide a cleaner surface than other insulators for "stanuing off" the arc during rundown.

In order to ensure an adequate gas flow over the entire insulator surface, the cylindrical shape of the old insulator shown in Figure 1 was tapered and rounded as illustrated in Figure 3. A 7 degree tapered configuration was designed to allow more gas flow around the "triple junction" point (interface of the metal, insulator, and vacuum-gas environment) and still maintain the same approximate length and thickness as the old insulator. The tapered design also allows the injection gas to flow preferentially along the inner electrode as opposed to the outer electrode, capturing more gas in the pinch. A

11
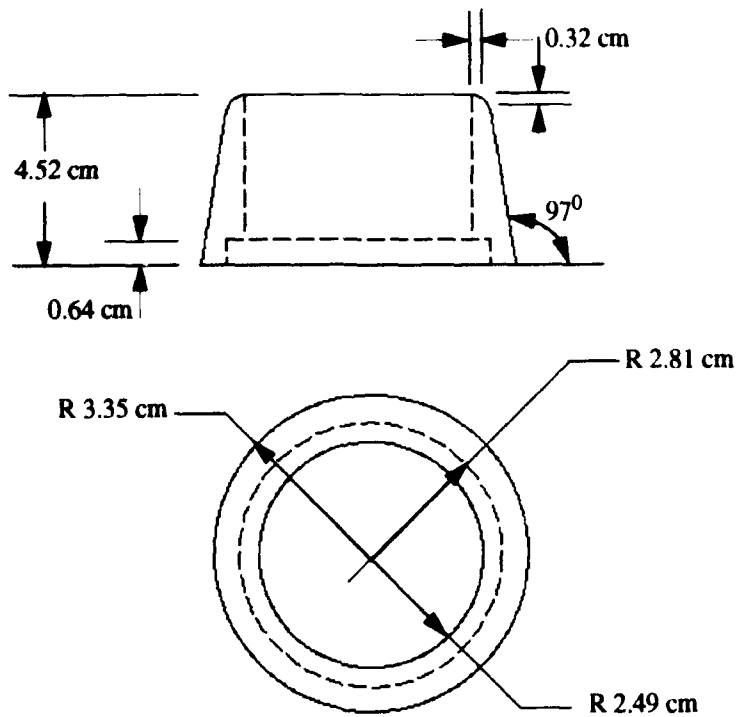
Figure 5. Ceramic Insulator Design

thickness of at least 0.32 cm of ceramic material was required for machining purposes, but this restriction limited the taper angle to 7 degrees maximum.

Control System / Timing Circuit.

Proper operation of gas puff injection requires the sequential opening of the gas valves and firing of the capacitor banks. The time intervals between each event must be precisely determined in order to properly operate and optimize the performance of the system. The short length of the time intervals requires an automatic timing system which can perform each event consistently. A guideline for the operation sequence of the gas-injected system is given later in the section "Control System Test."

A timing circuit, shown in Figure 6, was developed to operate the UI DPF with the new gas injection system. This timing circuit controls three peripheral devices: the Marx generator gas line solenoid which fires the system, the ring valve solenoids, and the electromagnetic switches which allow current flow to the axial magnetic field. Control of

12
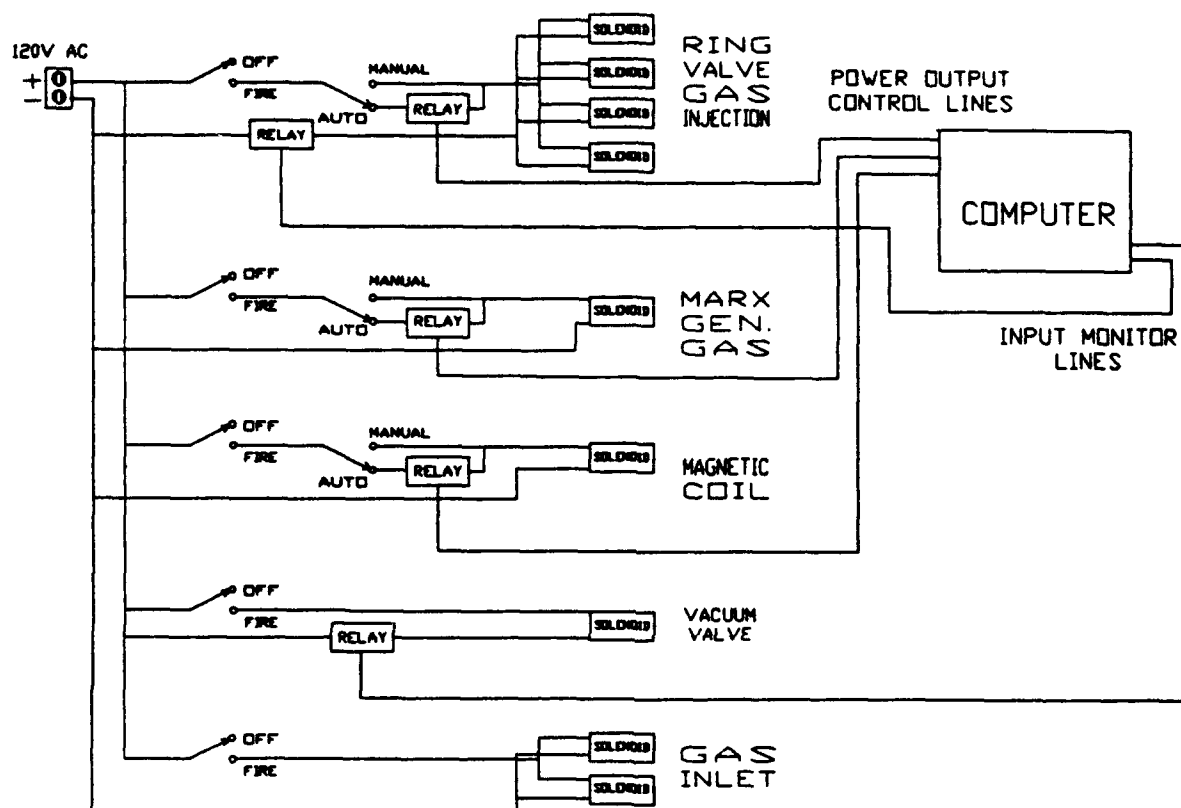
Figure 6. Gas Injection Timing Circuit Schematic

the peripheral devices is performed by three basic components of the timing circuit: the relay switches, the interface switches, and the PC 286 computer.

The relay switches consist of three Crystrom 6402A and two Crystrom 6201A circuits. Each 6402A circuit toggles a 240-Volt, 3-Amp AC current on and off based upon voltage signals received from the computer's Digital Analog Acquisition Card (DAAC). The 6201A circuit monitors the AC voltage status of a power line and sends voltage signals to the DAAC. A high voltage signal from the DAAC toggles the 6402A

circuit to OFF and corresponds to zero voltage on the 6201A circuit. Initially the 6402A circuits must be turned off by the computer when the timing circuit is run.

The interface switches are three manually operated toggle switches which allow manual or automated operation of the ring valve solenoids, the axial magnetic coil, and the Marx generator. The timing circuit allows automated firing of the focus for both modes of operation. When a switch is toggled in the manual position, the corresponding device can be operated manually without involving the relay circuit. Thus, if the timing circuit fails, the peripheral devices can be operated manually.

The computer controlling the relay circuits is an IBM 10 MHz model 5150 personal computer. The relay circuits are interfaced to a DAAC installed in the computer. A Fortran program named NU2 controls the firing sequence of the gas-injected system. (Appendix D presents this program.) A safety feature disables the system during each run if the electromagnetic vacuum valve is open or the ring valve solenoids are left on manual control. The program calls for input from the 6201A relay circuits which monitor the AC voltage status of the vacuum valve and the ring valve solenoid power lines. A low voltage signal from the circuits to the DAAC correlates to an ON power status in the AC lines. As the computer boots up the DAAC, output signals are all set low, which toggles all of the 6402A circuits high at the beginning of the program. All operation of the relay circuits is carried out in the program with the reverse logic described above.

The gas-injected mode of operation must be have precise control in order to work properly, and this requirement is well suited to computerized control. On the other hand, the pressurized chamber mode of operation can be run manually or controlled by the computer. Thus each peripheral device is wired in parallel to the relay switches and the interface switches. Each interface switch is wired in series with a manually operated ON/OFF switch. For computer operation of the focus, each interface switch is set to ON. Power to the peripheral devices is toggled on and off by the relay circuits. For manual operation the interface switches are set to manual and power to the peripheral devices is toggled on and off by the corresponding manual switch. At present, only the devices related to the fire control of the system have been automated. However the entire focus could easily be automated by installing additional relay circuits and interface switches, and by expanding the program.

The intervals for the timing circuit were determined experimentally. The time intervals are measured from sets of dual voltage measurements of the trigger signals from the computer to the relay circuits of a storage oscilloscope. The important events to be measured are the trigger signal to the Marx generator relay circuit and the discharging of the capacitor banks; the trigger signal to the ring valve solenoid relay circuits and the trigger signal to the Marx generator; and the trigger signal from the ring valve solenoid relay circuit and a piezoelectric pressure transducer (PPT) set at the breech of the gas-injection system.

14

A Rogowski coil exists on the transmission plate to the electrodes. This coil measures the change of current with respect to time, and outputs a voltage signal form this change. The voltage output from the coil is stored on the storage oscilloscope along with the voltage trigger signal from the computer to the relay circuit. The time interval between the events is measured from the stored image and used to set the approximate interval for the timing circuit program.

Similar measurements were performed on the time intervals for the opening of the ring valve. A piezoelectric pressure transducer is installed at the breech of the gas-injection system to measure the pressure of the gas flow into the system and to measure the pressure of the gas flow in the plenum. The pressure is calibrated in terms of voltage which can be measured on an oscilloscope. The critical pressure for the initiation of the arc is found from the Paschen curve. However, the pressure at which the system may be triggered is typically higher than the critical pressure due to the desire to inject larger amounts of gas for propulsion purposes. The desired voltage corresponding to this pressure is stored on the oscilloscope along with the voltage signal from the relay circuit. The intervals between events are then determined from the oscilloscope image.

The easiest measurement is the time interval between the trigger signal to the ring valve relay circuit and the trigger signal to the Marx generator relay circuit. Both signals are easily captured by attaching voltage probes to the circuit board.

Once all of these intervals are determined, the time values are used as starting points and small adjustments are made to optimize the system.

Benchtop Testing.

In order to test the operation of the new gas injection systems, the control system, and various associated components, a series of tests were undertaken. These were done as "benchtop" tests where each component was tested separately so that any problem could easily be isolated and corrected. The following sections discuss the tests and results performed on each separate unit.

Puff Valve.

Pressure tests on the plenum were performed to verify that an adequate mass flow could be contained. The mass between the electrodes corresponding to a static fill pressure of 3 Torr can be calculated from the Ideal Gas Law and the volume between the electrodes.

$$M = \frac{P_{ch}(Vol)}{kT} \frac{GMW}{6.023 \times 10^{23}} \tag{1}$$

Where:

M = Mass between the electrodes (kg)

P_{ch} = Pressure in the chamber (Pascal)

(Vol) = Volume between the electrodes (m^3)

k = Boltzman's constant (J/°K)

T = Temperature of the gas (°K)

GMW = Gram Molar Weight of the gas.

From the Ideal Gas Law the pressure in the plenum needed to give the same mass between the electrodes as in the static mode is given as:

$$P_{pl} = \frac{MkT(6.023 \times 10^{23})}{(Vol)_{pl}\ GMW} \tag{2}$$

Where:

P_{pl} = Pressure in the plenum (Pascal)

M = Mass between the electrodes (kg)

$(Vol)_{pl}$ = Volume of the plenum (m^3).

To test the puff valve, the chamber was initially evacuated to a base pressure of about 50 mTorr. The plenum pressure was then raised gradually and the puff valve was tested at each pressure increment. At 15.5 Torr of plenum pressure, i.e. "the critical pressure," the pressure gradient force became strong enough to fully open the puff valve. Critical pressure measurements were conducted at several chamber gas pressures, and the results were quite similar; the puff valve can operate satisfactorily as long as the pressure ratio between the plenum and the chamber is <300.

The gas valve and injection system described above was constructed for the 10-kJ DPF experiments. One objective of this work was to enable an easy scale-up to a larger focus such as the 1/4-MJ unit planned for the DPF in the future. In order to scale up to the 1/4-MJ unit, several issues have been considered, namely:

- achieving a faster rise time
- reduction of the influence of jitter in the Marx generator
- development of a prototype capable of a high repetition rate as is eventually desired in a practical thruster
- isolation of components from RF surges.

To study this, a computer model of the present injection system was developed and the results are reported later in Section "Puff Valve System Modeling." Results from the analysis described there indicate several improvements that will be included in the next upgrade to the experimental setup (see Section "Advanced Valve Concept").

Control System Test

Basic testing of the timing circuit was performed by operating individual components of the DPF with the timing circuit. Random time intervals were inserted into the code and operation of the corresponding components observed. The program NU2 was used to run the Marx generator, axial magnetic field, and ring valve in their proper time sequence. All test runs made were successful.

The success of these random time interval test runs on the timing circuit show the basic design to be trouble free. One limitation of the system is that the smallest time increment for the time intervals is one millisecond. This time limit originates in the IBM 5150 computer. If this becomes a problem, the replacement of a circuit board in the computer with a board with fast chips would decrease the time increment. Since the program can be used on any IBM compatible computer, installing it on a faster computer is also an option. The Fortran code used in this system is described in Appendix D.

Operation with the control in the static mode is very similar to operation of the system prior to installation of the gas injection system. The vacuum chamber can be pressurized from gas from the plenum. The ring valve is closed for the pulsing of the DPF in the static mode since leaving the ring valve open requires the use of the solenoid. The timing circuit is typically operated in the manual mode since no sequential operations are involved.

Operation of the system with the gas injection system requires a more complex series of actions which are controlled by the timing units. The operation sequence used in this case is as follows:

1) Vacuum chamber is pumped down to 0.1 mTorr.

2) Computer and electronics are turned on; desired timing sequence is programmed into the computer.

3) Ring valve is manually switched on to vacate residual gases in the plenum and then closed.

4) Gas line pressure to the plenum is set to desired pressure.

5) Vacuum chamber is pressurized with H_2 gas to protect insulator from misfires during charging.

6) Electronics are set to automatic status and desired timing intervals are set on the computer.

7) Capacitor banks and Marx generator are charged up.

8) Vacuum chamber is pumped down to 0.1 mTorr, and then vacuum valves are shut.

9) Computer timing program is initiated, firing the system.

10) The timing program resets.

11) Procedures 6-10 are repeated.

This control system is designed to make future upgrades easy. Modifications in the operation of the gas-injected system can be made as needed to match new experiments. A possible addition to the timing circuit would be the installation of a relay circuit which monitors the voltage on the banks and fires the system when a desired voltage is reached. At present, however, the system is easily fired manually when the desired voltage is reached.

Puff Valve System Modeling.

As described previously, tests have confirmed the operation of the puff valve. In preparation for future experiments which use gas puff injection, valve operation in the full DPF has been simulated with a computer code specially developed for this purpose.[7]

The injection system may be simulated as a reservoir connected to a large volume, initially at vacuum, through an orifice, an annular pipe and another orifice (see Figure 7) The flow system characteristics are listed in Table 1.

A constant solenoid force was assumed, although, in practice, some small variation from the data specified in the catalog is expected. The restrictor mass includes the connecting rods and the solenoid anchors. The dampening factor accounts for the air compression during the restrictor movement.

First, the flow regimes in the various segments of the flow system must be determined. During the injection cycle, the flow changes from molecular to intermediate to viscous in all segments. A major computational simplification results if the first two flow regimes are not included. Then the limits of the three flow regimes employed in the model become:

Flow Regimes	Condition	
Viscous	$\frac{Q}{D} > 200$	$\frac{D}{\lambda} > 110$
Transition	$\frac{Q}{D} < 100$	$1 < \frac{D}{\lambda} < 110$
Molecular		$\frac{D}{\lambda} < 1$

where D is the equivalent segment diameter in cm, Q is the total flow rate (Torr-lit/cm^2), and λ is the collisional mean free path.

18
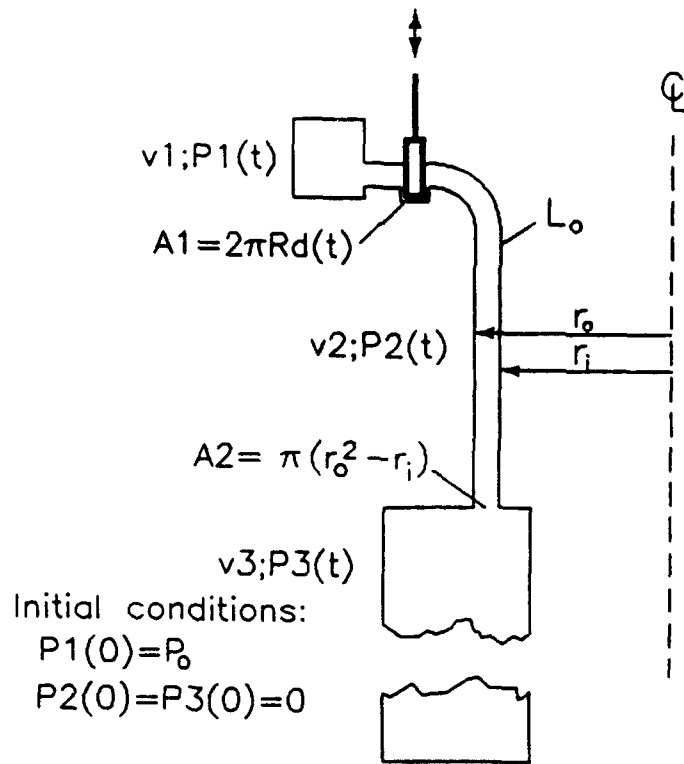
Figure 7. Flow Diagram for Gas Puff System.

With these inputs a simple model for the gas injection system is constructed. The viscous conductance C_v of a radial orifice is given by the approximate equation:

$$C_v = \frac{9.1A}{1 - \left(\frac{P_2}{P_1}\right)} \left[\frac{P_2}{P_1}\right] \left[\frac{2\gamma}{\gamma - 1}\left(\frac{T}{M}\right)\left[1 - \left(\frac{P_2}{P_1}\right)^{\frac{\gamma - 1}{\gamma}}\right]\right]^{0.5} \tag{3}$$

Here C_v is the conductance in Torr-lit/cm^2, and $P1$ and $P2$ are plenum and annulus pressures, respectively, $A = L_1\ d(t)$ is the orifice cross section while L_0 and $d(t)$ are the orifice circumference and gap, respectively, and M is the molecular weight of gas. Note that the gap spacing is a function of time. The gas conductance C_g the annular channel is given by the equation:

19

Table 1. DPG Gas Puff Injector Parameters

Flow System	
Cylindrical plenum volume	$150 \, cm^3$
Initial plenum pressure	50 Torr
Orifice circumference	22 cm
Annulus area and length	$7.4 \, cm^2$, 5.8 cm
Injection port area	$15 \, cm^2$
Inter-electrodes volume	$1200 \, cm^3$
Mechanical System	
Flow restrictor mass	0.5 kg
Spring constant (assumed)	5×10^4 N/m
Dampening factor (assumed)	0.1 N-s/m
Initial spring compression	1 mm
Initial O-ring compression	0.18 mm
Force - 4 solenoids	165 N
Maximum restrictor stroke	2 mm

$$C_g = 900 \, \frac{T}{M} \, \frac{P}{L} + \left[r_0^4 - r_i^4 - (r_e^2 - r_i^2) \log\left(\frac{r_0}{r_i}\right) \right] \qquad (4)$$

where r_0, r_i, and L are the outer radius, inner radius and annulus length respectively. The viscous conductance C_3 of the annulus end facing the inter-electrode gap is found from equation (3). The total flow system conductance C_T is calculated from the discrete C values:

$$C_T = \frac{1}{\displaystyle\sum_{i = v, g} \frac{1}{C_i}} . \qquad (5)$$

The pressures at the three sections are calculated by integrating the net flow rate through each section.

To complete the model, the annulus exit pressure is back calculated from the flow rate through the exit orifice. The gap spacing $d(t)$ is calculated by integrating the differential equation for the mass-spring system of the flow restrictor, with the initial conditions specified in Section "Estimates for Modified DPF" in Table 2.

$$\frac{dx}{dt} = M_r \frac{d^2x}{dt^2} + C \frac{dx}{dt} + K \cdot x(t) = F(t) \tag{6}$$

A Fortran code has been constructed to simulate the pressure history in each segment.[7] The volume circumscribed by the electrodes is taken as a closed segment. This is a good assumption since the injection period is smaller than the gas flow time.

Results from the simulation are shown in Figure 8. It is seen that an initial pressure peak in the annulus results when the limiting chocked flow occurs at the injection port. After 7 ms transience, all segments reach pressure equilibrium. Thereafter, equilibrium flow continues smoothly.

These results confirm the operational capability of the design. However, to study further optimization, a parametric study was conducted, starting with the valve opening time set to about 250 μs (simulating an arbitrary quick valve). As seen in Figure 9, the injector response time is longer than 1 ms, even if the annulus segment reaches pressure equilibrium within a few 100's μs. In other words, the present design is best suited for low rep-rate operation. Additional tuning would be required to extend the design to high rep-rate operation. This can be achieved by adjusting, or replacing, the solenoid tension spring. Another option which could result in a more versatile high rep-rate valve would be to design a comparatively new, advanced version of the valve. This possibility is briefly discussed in the following Section "Advanced Valve Concept." Since high rep-rate operation is not an immediate objective, however, the present spring setting has been retained for current runs.

Some additional improvements would be desirable when high rep-rate operation is added later. The present Marx generator jitter (15 ms) plus the injected gas mass and timing variations limit operation of the present arrangement to 20 Hz.

The random phase effect could be partially corrected by connecting an appropriate capacitor (50 μf for 200 mH) in series to each solenoid or by using a dedicated pulsed power supply. The Marx generator jitter could be eliminated by one of the following routes:

- Trigger the Marx generator spark gap with an auxiliary small SCR/ferrite circuit.[8]

- Replace the Marx generator with the thyratron/capacitor bank (30 kV, 0.03 μf) cabinet. This device seems to have sufficient energy to trigger the main spark gaps. The peak output voltage could be amplified, if required, by using a double coaxial cable arrangement.[9]

21
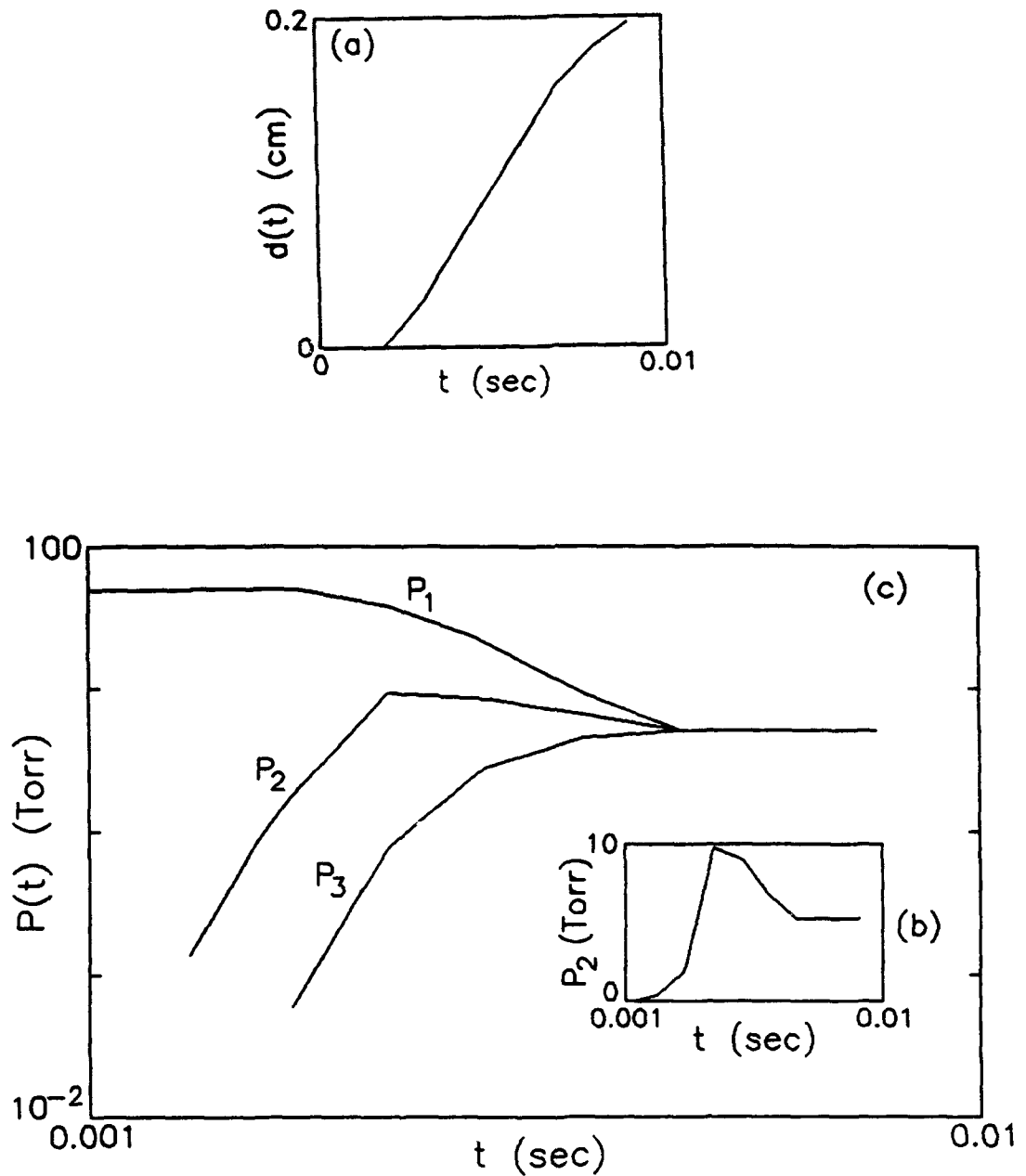
**Figure 8.** Gap Spacing and Pressure Histories in the Present UI Flow Systems

(a) restrictor orifice gap spacing as a function of time

(b) annular channel pressure (linear)

(c) pressure histories in all sections (logarithmic)
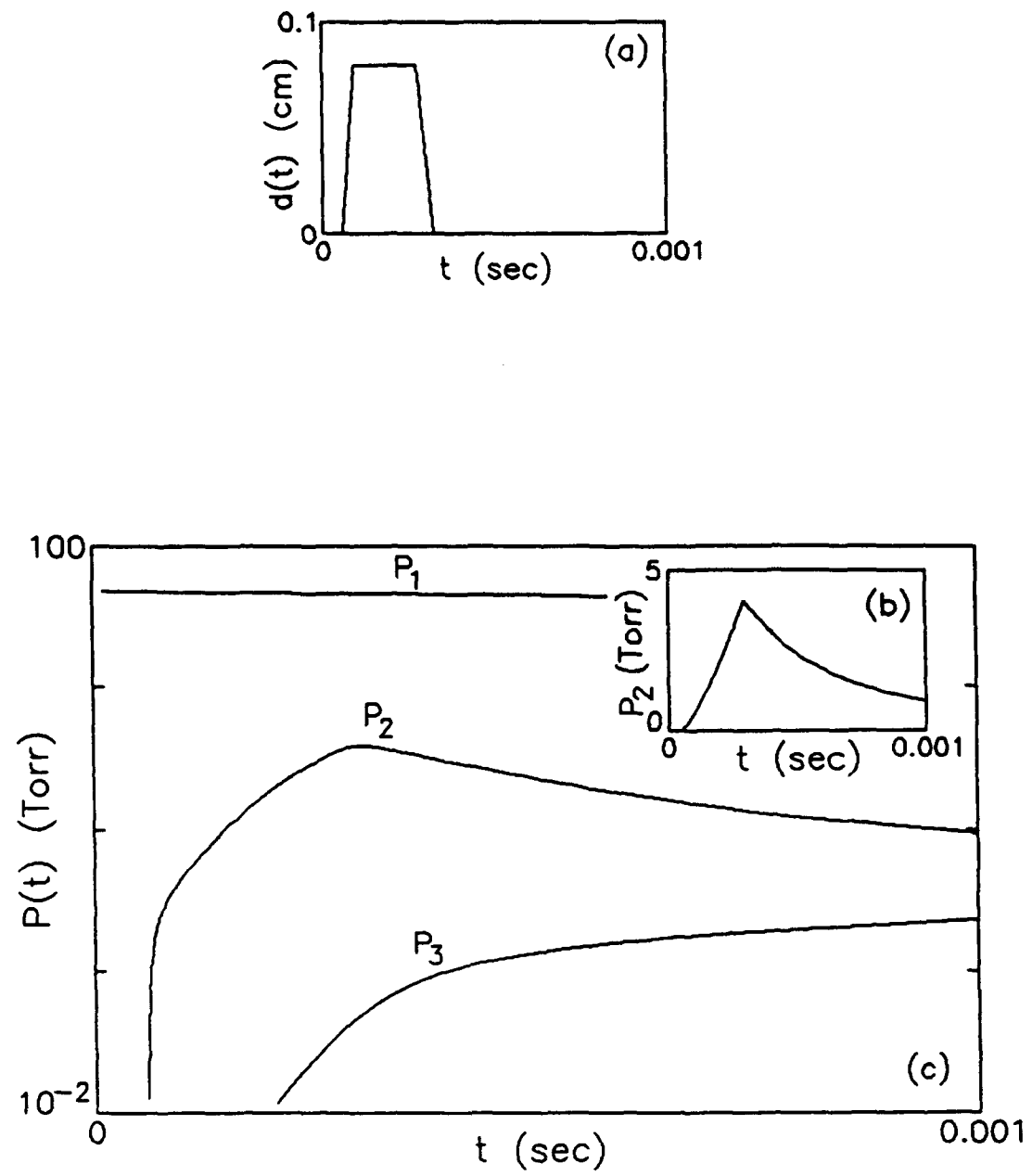
Figure 9. Pressure Histories in the Hypothetical Piezo-motor Valve

    (a) valve opening

    (b) annular channel pressure (linear)

    (c) pressure histories in all sections (logarithmic)

An upgrade of this type will be undertaken after the next series of low rep-rate experiments is complete.

In summary, the present gas injection valve has successfully passed extensive bench tests. In addition, the simulation studies described in this section confirm its operation in a low rep-rate DPF as designed for next-step thrust measurements. Various modifications to achieve high rep-rate operation have been explored in anticipation of later experiments.

Advanced Valve Concept.

The present valve is suitable for low rep-rate operation. However, an advanced gas puff system design would be needed for >1 kHz operation. One requirement is to be able to increase the gas pressure in the plenum, and the charging rate, without changing the mass of the stored gas.

One interesting approach is suggested by Sato, et al., who describe a 1 kHz magnetically insulated diode.[10] A pre-determined amount of gas is first admitted into the plenum using a foil diaphragm. In turn, the gas is inductively broken down so that the resulting MHD force accelerates gas injection throughout, enabling a fast repetition rate.

The present computer controlled timing circuit developed by the DPF group is a powerful instrument that could be adopted to any gas puff injection scheme. However, a lesson to be learned is the danger of strong RF noise associated with the DPF system[10] An optical isolator could be installed between the computer control cables and the injection system to protect it against RF surges. This seems especially desirable at higher bank energies.

Estimate of Propulsion Enhancement

Introduction.

Thrust is provided by the rundown of the gas between the electrodes and by the energetic fusion products (alpha particles and protons) in the pinch. Fusion products and the associated plasma can be directed outward through a magnetic nozzle. By pursuing such a system at a high rate, thrust is produced in a quasi-steady-state fashion.

Prior Performance Estimates.

Use of the DPF as a space propulsion device would require operating the system in a gas-injected mode. Indeed, the modifications to the UI DPF described in the earlier sections were done to allow small scale testing of such operation with the UI DPF. An analogous mode of operation has been performed before in experiments on coaxial

plasma guns operating in the deflagration mode.[11] However, these experiments provided plasma acceleration but not a pinch i.e., added fusion energy, as envisioned in a DPF. The outer electrode at the UI DPF is constructed of 24 rods which, when operated in a pressurized chamber, results in a faster arc rundown than a solid outer electrode estimated to be ~3×10^5 m/s based on previous work on the UI DPF[12]. Then, if the pulse rate is increased to 10^4 pulses per second, a total thrust of 200 Newtons is possible. (Note that due to limitation of the 1 mSec time interval, imposed by the computer, the pulse rate can only be increased to 10^3 pulses per second in practice). Velocity measurements made on coaxial plasma guns in the deflagration mode show a particle velocity of 10^6 m/s.[13] Operating the DPF in the gas-injected mode with the more efficient electrode design described here should increase the rundown particle velocity by a factor of 10 to 100 and also give better fusion performance in the pinch. This would provide a minimal total thrust of 2000 Newtons (430 lbs.) for a system operated at 10^4 pulses per second.

Estimations of the thrust for a scaled-up version of a DPF have been made by Mead.[14] If the system has a total capacitance of 10^{-3} to 10^{-4} farads and is charged to a voltage of ~100 kV, a maximum current greater than 10^7 Amp is achievable. At this amperage, gas at a density of 0.005 kg/m^3 can be rundown and pinched to a density of 4.3×10^{22} cm^{-3} and temperature of 100 keV, giving a thrust of 9.49 Newtons per pulse. If the system is modified to pulse at 10^4 per second, a total thrust of 93,900 Newtons (20,400 lbs.) is predicted, providing a most attractive propulsion unit.

This estimate of the thrust is based on the key assumption that the temperature in the pinch scales as the square of the current.[15] While this scaling law has been experimentally verified for systems up to ~1 MJ in a conventional DPF,[6] there is no experimental evidence that it holds at the high energies required for the scaled-up version of the DPF operating in the gas-injected mode. Likewise, previous theory and data accumulated for coaxial plasma guns only relate to the rundown phase of operation for the DPF.[16] There exists no theory at the present time to couple the plasma formed during the rundown phase of operation to the plasma formed in the pinch from the collapse of the arc. Finally, it is important to recognize that while the DPF is similar in many respects to a coaxial plasma accelerator or a magnetic plasmoid accelerator, the added fusion energy supplied by the pinch step greatly enhances the energy efficiency.

Estimates for Modified DPF.

As a guide to future experiments, we have carried out some preliminary studies of the use of the modified DPF in space propulsion. Using a scaled-up model. From this model, the contribution of fusion energy to thrust and specific impulse is estimated.

The DPF model consists of two parts: rundown and pinch. During the rundown phase, the gas between the electrodes is ionized and a fraction swept forward (rundown mass) by the current sheath. The electrode lengths are set such that when the current sheath reaches the end, the current delivered by the capacitor banks is at a maximum. (If the current does not reach an absolute maximum during the rundown, the electrode length

$$R_L$$

$$I(t)$$

$$L = L_0 + \dot{L}t$$

$$U(t)$$
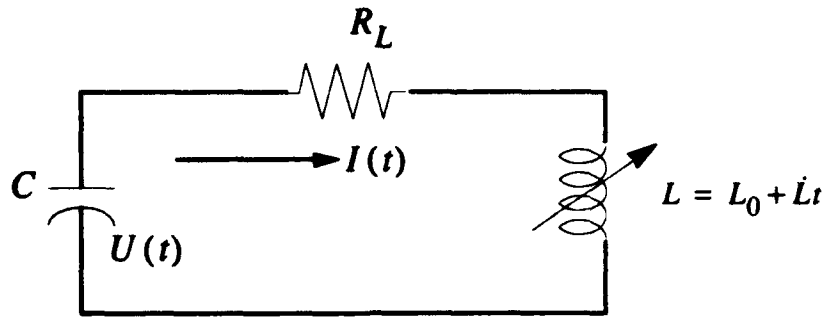
Figure 10. DPF Rundown Circuit

is set such that the current at the end is an arbitrary fraction of the local maximum current, say 80%.) A fraction of the rundown plasma is then trapped in the pinch phase, while the remainder is exhausted axially.

In the pinch phase, the trapped plasma is constricted by the magnetic field of the current at the end of the electrodes (maximum). The compressed plasma is heated like an ideal gas to fusion temperatures, with a Maxwellian energy distribution assumed. Fusion reactions occur at a rate corresponding to the density and temperature of the fuel plasma, with the accompanying energy release going to heat the rocket propellant.

During the rundown phase, the DPF is approximated by an RLC circuit, depicted in Figure 10, with the inductance increasing at a constant rate[17]

The time rate of change of the inductance, $\dot{L}$, is proportional to the plasma rundown velocity, experimentally determined to be roughly constant.

$$\dot{L} = v_{run}\frac{\mu_0}{2\pi}ln\left(\frac{r_c}{r_a}\right) \tag{7}$$

where r_c and r_a are the cathode and anode radii, respectively.

Solving for the charge on the capacitor as a function of time, $q(t)$, a series solution, was obtained:

$$q(t) = \sum_{n=0}^{\infty} A_n \, t^n \tag{8}$$

26

$$A_0 = \frac{2W}{U_0} \tag{8a}$$

$$A_1 = 0 \tag{8b}$$

$$A_2 = -\frac{\dot{i}_0}{2} \tag{8c}$$

$$A_{n+2} = -A_n \frac{U_0 \dot{i}_0}{2W} \frac{1}{(n+1)(n+2)}$$
$$- A_{n+1}(R_l + \dot{L}(n+1)) \frac{\dot{i}_0}{U_0} \frac{1}{(n+2)} \tag{8d}$$

where W, the capacitor bank energy, $\dot{i}_0$, the initial rate of current change, and $\dot{L}$ are held constant. This solution is a polynomial in t; the recursion relation for coefficients A_3 and above is also given.

The voltage on the capacitors is proportional to the charge, and the current delivered as a function of time is simply the negative time derivative of the capacitor charge.

$$U(t) = \frac{q(t)}{C} = \frac{U_0^2}{2W} q(t) \tag{9}$$

$$I(t) = -\frac{d}{dt} q(t) \tag{10}$$

The impedance of the plasma focus rises sharply when the pinch begins. This model assumes a jump in the pinch inductance and resistance at the beginning of the pinch, but assumes that the pinch impedance remains constant during the stable pinch lifetime. Figure 11 shows the equivalent circuit for the DPF during the pinch phase. The solutions are for a RLC circuit.

The pinch is approximated by a cylindrical plasma, whose dimensions remain constant during the stable pinch lifetime. To maintain plasma pinch dimensions, magnetic pressure at the plasma edge must balance the kinetic pressure of the plasma.

$$\frac{\mu_0 I^2}{8\pi^2 r_p^2} = nkT \tag{11}$$

27
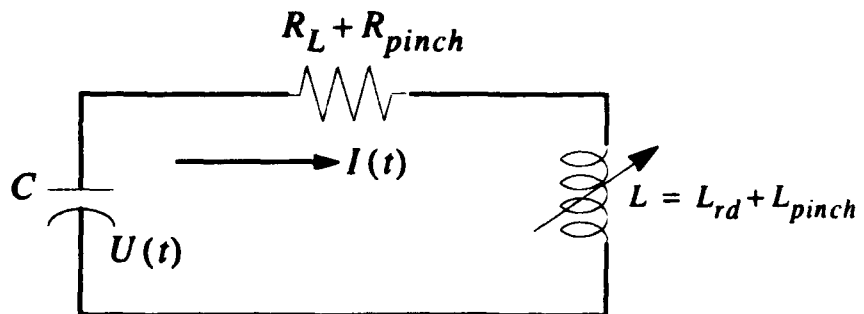
Figure 11. DPF Pinch Phase Circuit

where r_p is the pinch radius, $n = n_i + n_e$ is the particle number density in the pinch, and kT is the particle energy. The pinch becomes unstable when current is no longer delivered from the capacitors $(U = 0)$, and thus the magnetic field drops to zero.

The fill gas density is set to provide the maximum reaction rate for the maximum current delivered to the pinch. If one treats the pressure in the pinch as fixed by the induced magnetic field from the maximum current, then there exists plasma temperature for which the reaction rate is a maximum. In the plasma, the reaction rate is proportional to the square of the fuel density and the reaction rate parameter, $<\sigma v>$. The reaction rate is maximized when $<\sigma v>/(kT)^2$ is maximized. For D-^{3}He, this occurs at $kT \approx 47$ keV.

Shown in Figure 12 are the relative voltage and current profiles as a function of time during the rundown and pinch phases for bank energies of 250 kJ and 100 MJ. Note that for the 250 kJ case, the voltage and current profiles follow expected trends. For the 100 MJ case, the pinch lifetime is very short, so the steady decrease in current occurs very quickly.

W=0.25 MJ
U0=08 kV
Imax=1.5 MA
i0=1e12 A/s
L=20 mΩ
RL=1.5 mΩ
Rpin=0.1 Ω

(a)

W=100 MJ
U0=212 kV
Imax=165 MA
i0=1e13 A/s
L=1 mΩ
RL=1.5 mΩ
Rpin=0.1 Ω
Q=19.3
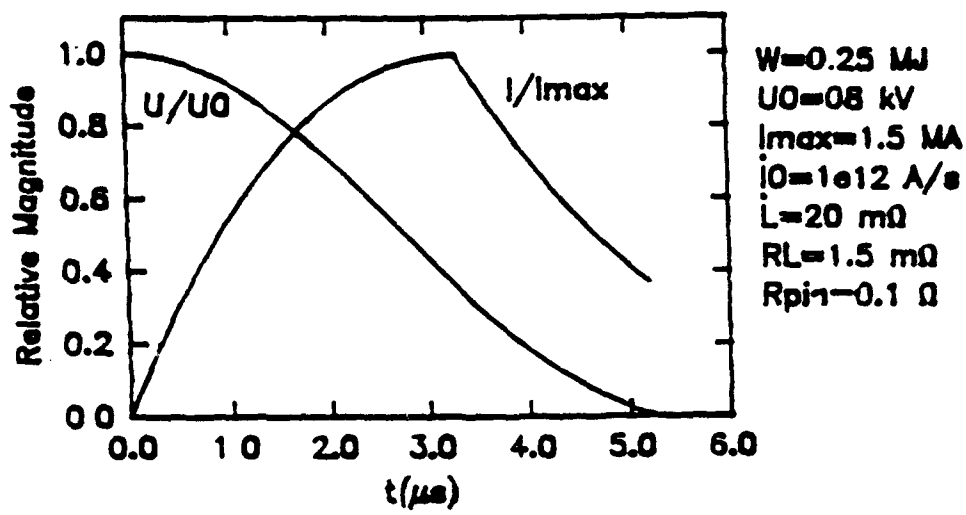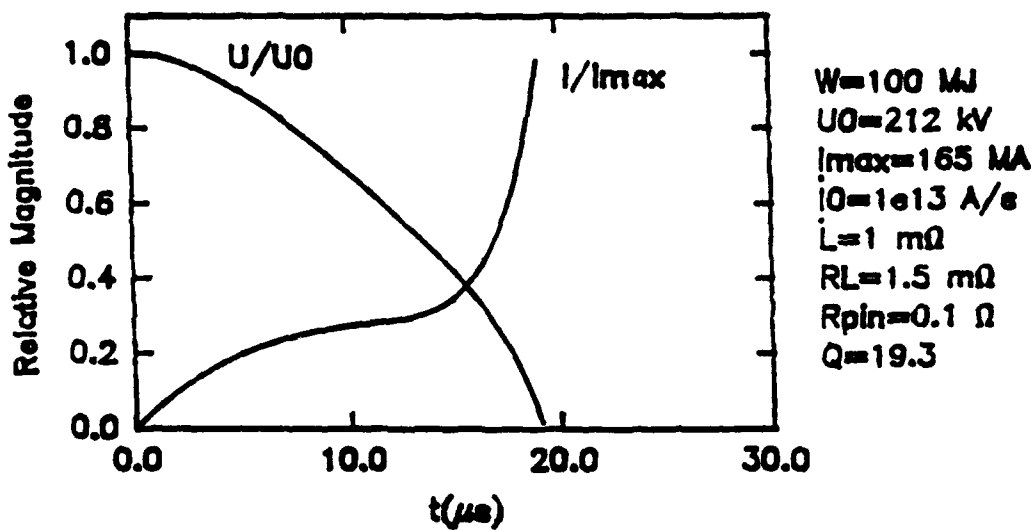
(b)

Figure 12. DPF Voltage and Current Profiles
(a) 250 kJ
(b) 100 MJ

29

Table 2. Q Values and Other Data from Several Cases $R_L = 1.5m\Omega$, $R_{pin} = 0.1\Omega$

Bank Energy (MJ)	0.25	1	10	100
$U_0 (kV)$ $\dot{L}(m\Omega)$	98 20	156 20	98 1	212 1
$I_{max}(MA)$ $E_f(MJ)$ Q	1.5 9.7 J 1	2.3 96 1	77 9.3 1.9	165 1830 19.3

The fusion energy produced during one pulse, E_f, is the integral of the instantaneous fusion power over the pinch lifetime. The total energy out per pulse is the sum of the bank energy, W, and the integrated fusion power, E_f. We can define the gain Q as the total energy out over the input energy.

$$Q \equiv \frac{E_f + W}{W} \qquad (12)$$

The fusion contribution to rocket performance is determined by comparison of thrust and specific impulse (or jet power) when the fill gas is a fusion fuel (D-^{3}He) versus when it is inert (H-^{4}He). If the majority of the energy from the pinch (all in charged particles) can be converted to useful thrust, then the DPF at higher bank energies looks promising indeed. The ratio of rocket performance with and without fusion contribution, is equal to the ratio of energy output, with and without fusion fuel. This is termed the Q value, and calculated Q values are presented as a function of the DPF bank energy in Table 2. At bank energies less than 1 MJ, the pinched plasma conditions are not sufficient to produce a measurable addition of fusion energy. For higher bank energies, a noticeable addition occurs. At 100 MJ, the added fusion energy results in a Q value of 20, i.e. the added fusion energy results in a 20-fold increase in jet power. This provides the opportunity for a significant increase in rocket performance. The added jet power comes with the added weight due to the DPF bank. However, as other studies show, the resulting power-to-weight ratio is still significantly enhanced over the comparable case where an inert fill gas is used, requiring a larger power source to provide it with the added jet power.

When these results are compared to other electric propulsion devices, which neither use fusion fuels nor provide any energy multiplication whatsoever, the DPF appears to be an excellent candidate for space propulsion.

Diagnostics.

Measurement of the thrust predicted for the experimental device requires highly sensitive, low noise diagnostics. A variety of possible thrust measurement techniques have been studied for other thrusters (ion, plasma, etc.)[18][19][20], however only some of these methods are suitable for the low thrust levels expected in the next step plasma focus experiment. The two most promising approaches appear to be the knife-edge ballistic pendulum and the "Piezoelectric Polymer PVDF Shock Guage".[21]

Conclusion

The design and construction of a gas injection system was completed for the UI DPF. The development of such a system is viewed as essential for future DPF applications to space propulsion.

Benchtop tests of the gas puff valve and control systems confirm that the new injection system alone functions as designed. A series of computer analyses of impedance matching characteristics of the inner electrode shape were carried out to select the optimum electrode design for use in the gas injected mode. The final design selected yields the optimum current delivery to the pinch. The resulting DPF system, with an integrated gas injection electrode and control unit, should provide a key device for testing the performance of this mode of operation for space propulsion.

As a guide to thrust experiments, we also developed a computer model of the modified DPF. Application of this model to scaled-up DPF units confirm the expectation that this type of thruster would be highly attractive if the technological development succeeds as anticipated. Theoretical scaling studies suggest that fusion energy in the pinch can provide additional energy for propulsion, but that the addition only becomes appreciable when the capacitor bank energy exceeds ten megajoules.

Publications Under Contract

- Barnouin, O., Temple, B., Miley, G.H., "Use of a Dense Plasma Focus as an X-Ray Irradiation Facility," *IEEE Intern. Conf. on Plasma Science*, 4P2-13, 190, Oakland, CA, May 21-23, 1990

- Temple, B., Barnouin, O., Miley, G.H., "Plasma Focus Device for Use in Space Propulsion," *Fusion Tech.*, 19, 846-851, 1991

- Miley, G.H., Barnouin, O., Temple, B., "Detection of Reaction Products Induced in Plasma Focus Electrodes," *Proc. Anomalous Nuclear Effects*, Provo, Utah, October 22-24, 1990

- Nachtrieb, R., Barnouin, O., Temple, B., Miley, G.H., Leakeas, C.,Choi, C.K., Mead, F., "Computer Model for Space Propulsion Using Dense Plasma Focus," *18th IEEE Intern. Conf. on Plasma Science*, p. 155, Williamsburg, VA, June 3-5, 1991

- Miley, G.H., Nachtrieb, R., Nadler, J., "Use of a Plasma Focus Device for Space Propulsion," *AIAA/NASA/OAI Conf. on Advanced SEI Technologies*, AIAA-91-3617, Cleveland, OH, September 4-6, 1991

- Temple, B.A., "Design of a Gas Injection System for the Dense Plasma Focus,"M.S. Thesis, Nuclear Engineering, 1992

References

[1] Froning, H.D., Mead, F., "Propulsion for Rapid Transits Between Earth and Mars," *Case for Mars IV International Conference*, 1990.

[2] Vernon, M.E., "Design, Construction, and Diagnostics of a Dense Plasma Focus," Master of Science Thesis, Department of Nuclear Engineering, University of Illinois at Urbana-Champaign, 1979.

[3] Temple, B., Barnouin, O., Miley, G.H.,"Plasma Focus Device for Use in Space Propulsion.", Ninth Topical Meeting on the Technology of Fusion Energy, Oak Brook, IL 1990.

[4] Degnan, J.H., et al, "Puff-Gas Coaxial-Injected Electromagnetic Coaxial Plasma Gun.",*J. Applied Physics* , 61(8), p.2763-2770.

[5] Warren, S.W.R., et al, "High-Energy Photon Spectra from a Coaxial Gas-Puff Experiment.", *J. Applied Physics*, 61(8), p.2771-2777.

[6] Herold, H., et al, "Comparative Analysis of Large Plasma Focus Experiments Performed at IPF, Stuttgart, and at IPJ, Swierk," *Nuclear Fusion*, 29, p.1255, 1989.

[7] Kislev, H. and Miley, G.H., "Gas Puff Valve for Dense Plasma Focus Thruster," Project Report RTA-PF-03, Rockford Technology Associates, Champaign, IL, 1991.

[8] Lindemuth, I.R., "Two-Dimensional Ablation in the Solid-Deuterium Z-pinch," *Phys. Rev. Let.*, 65(2), p.179-182, 1990.

[9] Lindemuth I.R., McCall, G.H., and Nebel, R.A., "Fiber Ablation in the Solid Deuterium Z-Pinch," *Phys. Rev. Lett.*, 62(3), p.264-267, 1989.

[10]Sato, T., Ochiai, I., Kato, Y., and Murayama, S., "High-Frequency Oscillations of Current and Voltage in a Plasma-Focus Discharge Device," *Rev. Sci. Instrum.*, 62(6), p.1504-1510, 1991.

[11] Michels, C.J., Ramins, P., "Performance of Coaxial Plasma Gun with Various Propellants," *Phys. Fluids Supplement*, p.S71, 1964.

[12]Venneri, F., "X-Ray Analysis of the Dense Plasma Focus," PhD Thesis, Department of Nuclear Engineering, University of Illinois at Urbana-Champaign, 1988.

[13]Cheng, D.Y., "Plasma Deflagration and the Properties of a Coaxial Plasma Deflagration Gun," *Nuclear Fusion*, 10, p.305, 1970.

[14]Mead, F., (Edwards Air Force Base, CA), private communication, June, 1990.

[15]Mather, J.W., "The Dense Plasma Focus," in *Methods of Experimental Physics*, Volume 9B, Academic Press, New York, p.187, 1971.

[16]Ashby, D.E.T.F., "Energy Loss in Pulsed Coaxial Plasma Guns," *AIAA Journal*, 3, p.1045, 1965.

[17]Decker, G., et. al, "Neutron Emission Parameters in Plasma Focus Devices," *Plasma Physics and Controlled Nuclear Fusion Research Conference Proceedings*, Vienna, Vol. 2, IAEA, p.136-142, 1978.

[18]Komurasaki, K., Arakawa, Y., "Hall Current Ion-Thruster Performance.", *Journal of Propulsion and Power*, Vol.8, No. 6, 1992.

[19]Yosikawa, T., Kagaya, Y., Tahara, H., "Thrust Measurement of Quasi-Steady MPD Arcjet.", AIAA-85-2003.

[20]Haag, T.W., "Thrust Stand for High-Power Electric Propulsion Devices.", *Rev. Sci. Instrum.*, 62(5), p.1186-1191, 1991

[21]Bauer, F., Graham, R.A., Lee, L.M., Samara, G., "Piezoelectric Polymer PVDF Shock Guage: State of the Research Art.", 39th Aeroballistic Range Association (ARA), Albuquerque, NM, 10-13 October 1988.

Appendix A
UI DPF Facility

The following pages are excerpted from a brochure explaining the UI DPF facility, entitled *Photographic "Tour" of the Dense Plasma Focus Facility, University of Illinois Fusion Studies Laboratory, Nuclear Engineering Program, University of Illinois, Urbana, Illinois 61801*, May, 1992.

UIUC DPF

The University of Illinois Dense Plasma Focus (UI DPF) is a unique pulsed power device used to produce high temperature dense plasmas during a pulse lasting 100s of ns. Uses range from X-ray production for solid state studies to plasma propulsion.

The focus uses Mather-type electrodes and a set of 20 x 2-μf capacitors in parallel (40 μf total capacitance) arranged in four perpendicular arms. The capacitors are discharged simultaneously by triggering four Trigatron spark gaps coupled to a 5-ns rise time Marx generator. The current has been measured to be 3-5 x 10^5 A. Peak temperatures of 1 keV and densities of 10^{19} cm^{-3} are achieved during the pinch. Further data can be obtained in the references listed at the end.

Figure 1 shows the capacitor bank arms and transmission plate. The cables at the top of the figure connect the Trigatron spark gaps to the Marx generator. Figure 2 shows a profile view of the DPF from behind the concrete shield. The capacitor charging equipment is shown at the right of the photo. The ceramic insulator, shown in Fig. 3, provides the plasma breakdown path between the inner and outer electrodes, shown in Fig. 4.

The inner and outer electrodes are connected to

Figure 2. Charging Equipment

the upper and lower transmission plates (installation shown in Fig. 5). A vacuum chamber encloses the electrodes and provides ports for diagnostics (Fig. 6).

Equipment and Diagnostics

The diagnostics used for the UI DPF include:
* Rogowski coil
* B-dot probes
* X-ray spectrometer
* Pinhole camera
* Nitrogen laser interferometer
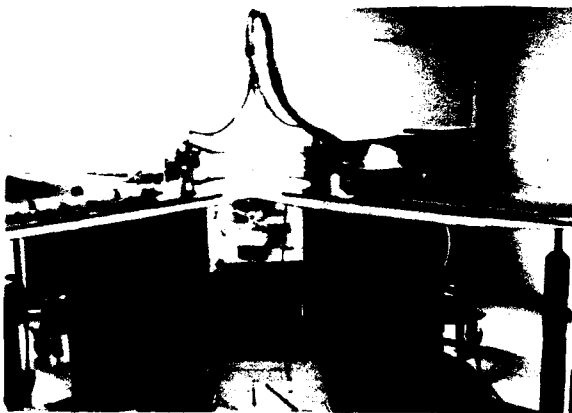
Figure 1. Layout of Capacitor Banks and Transmission Plates

Figure 3. Closeup of Ceramic Insulator
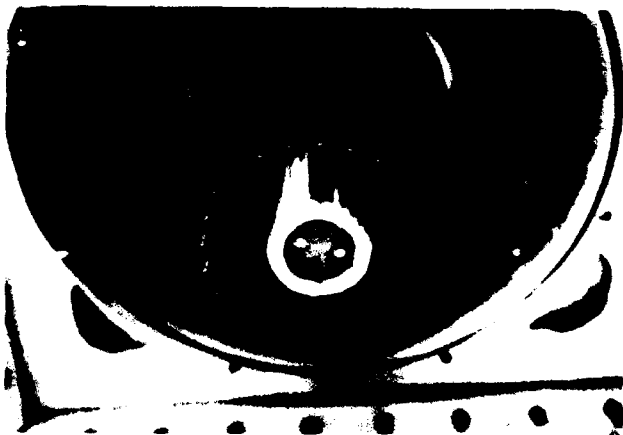
Figure 4. Squirrel-Cage Cathode and Inner Anode

Possible dia⌐ ıostics to be added include:
- Doppler sh⌐ measurement of plasma velocity
- Thruster plate
- Piezoelectric pressure transducer

The electromagnetic-shielded diagnostics cage holds the Personal Computer-controlled timing circuit and oscilloscope, shown in Fig. 7.

Figure 6. Vacuum Chamber In Place and Connected to Roughing Pump,Deuterium Lines

Figure 5. Jalal Javedani and Brian Temple Installing the Outer Electrode

Figure 7. Shielded Diagnostics Cage with Personal Computer Timing Control

Appendix B
Inner Electrode Designs and Inductance Graphs[1]

Electrode geometries with different impedances were considered. Figure B-1. provides a table of the various geometries analyzed. Results from calculation to analyze the inductance vs. axial length for the various designs are summarized in Figure B-2. through Figure B-4. Corresponding axial velocity calculations as a function of time are given in Figure B-5. through Figure B-7. Electrode design #41 was selected for initial use in the DPF due to its low inductance and high axial velocity.

1. Excerpted from: Temple, Brian A. "Design of a Gas Injection System for the Dense Plasma Focus." Masters Thesis, Department of Nuclear Engineering, University of Illinois at Urbana-Champaign, Urbana, IL, 1992.
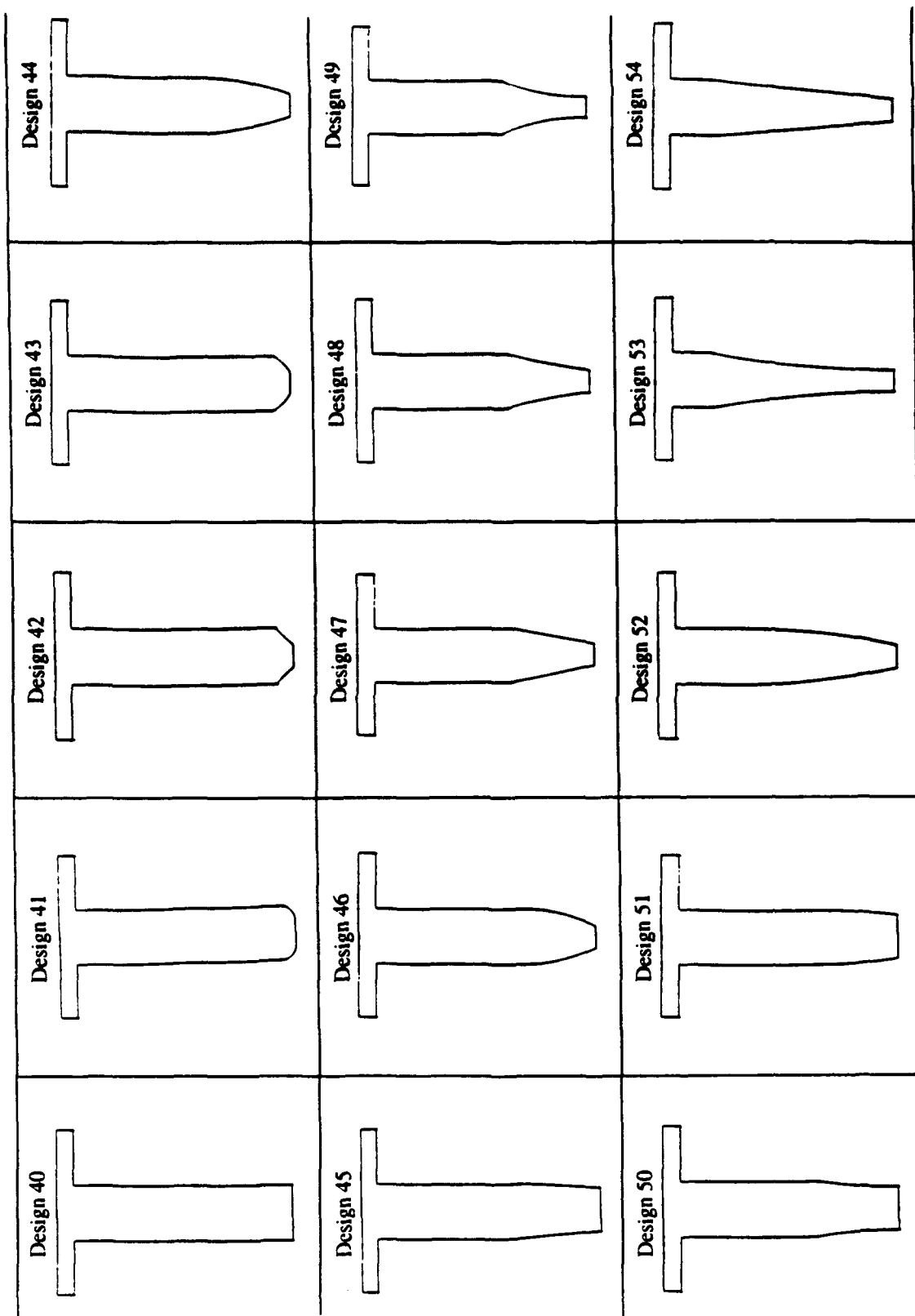
Figure B-1. All Inner Electrode Designs Considered. Design 41 proved to have the best properties. For dimensions, see Figure 2.

39
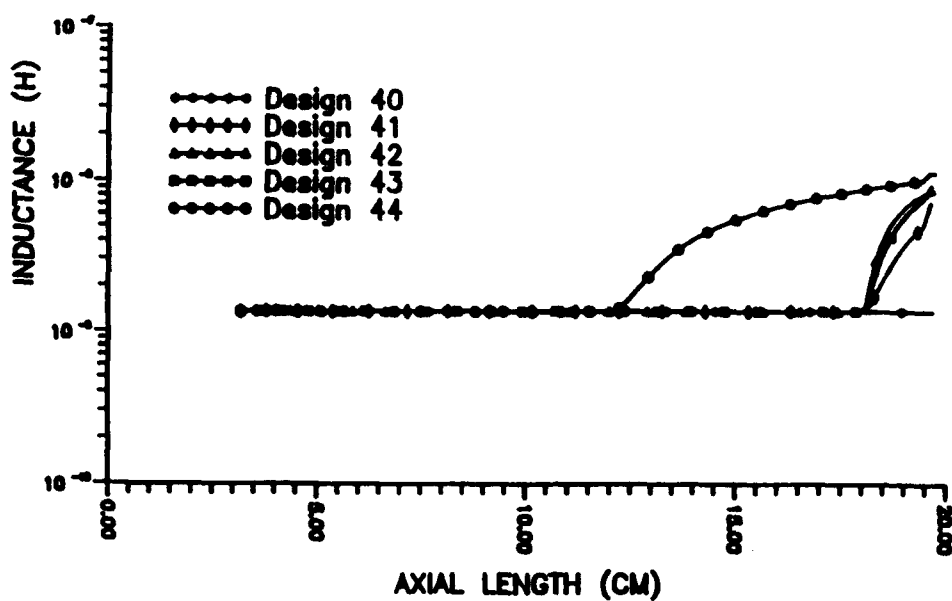
Figure B-2. Graph of Electrode Inductance vs. Electrode Axial Length for Designs 40-44
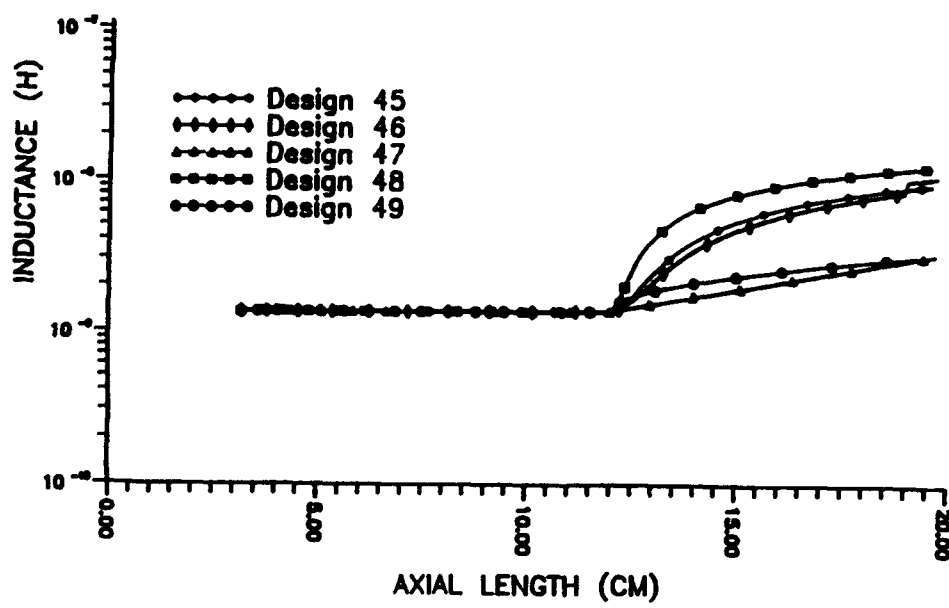
Figure B-3. Graph of Electrode Inductance vs. Electrode Axial Length for Designs 45-49
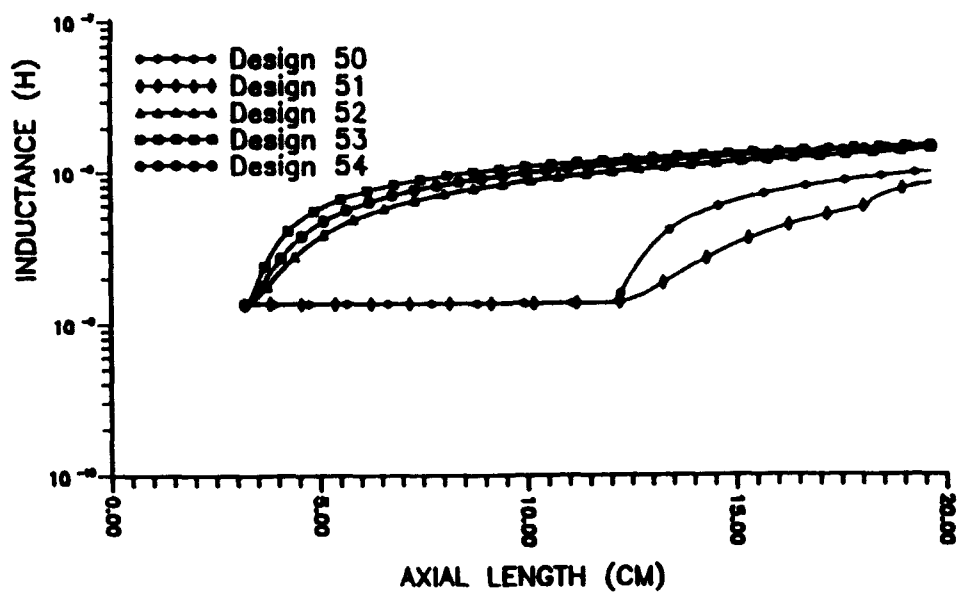
Figure B-4. Graph of Electrode Inductance vs. Electrode Axial Length for Designs 50-54
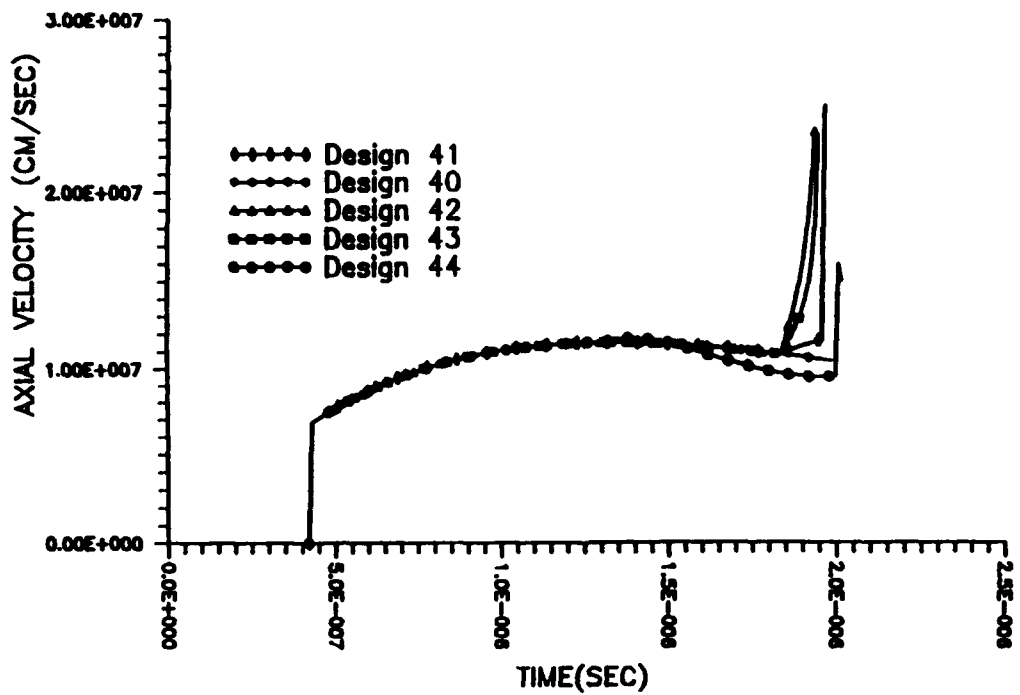
Figure B-5. Graph of Axial Velocity vs. Time for Designs 40-44

41
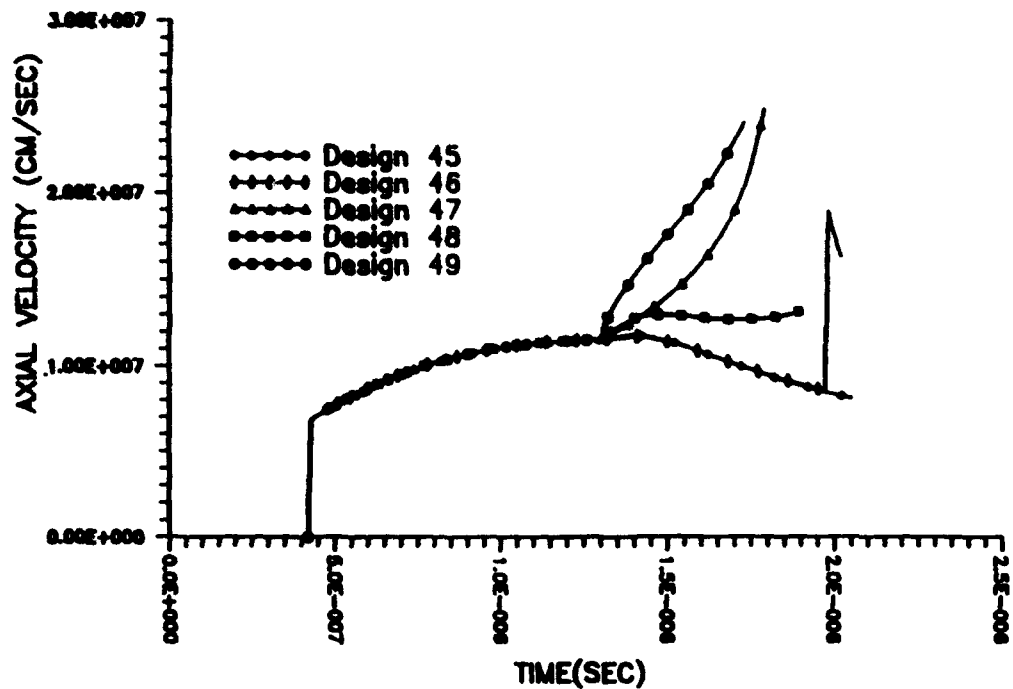
Figure B-6. Graph of Axial Velocity vs. Time for Designs 45-49
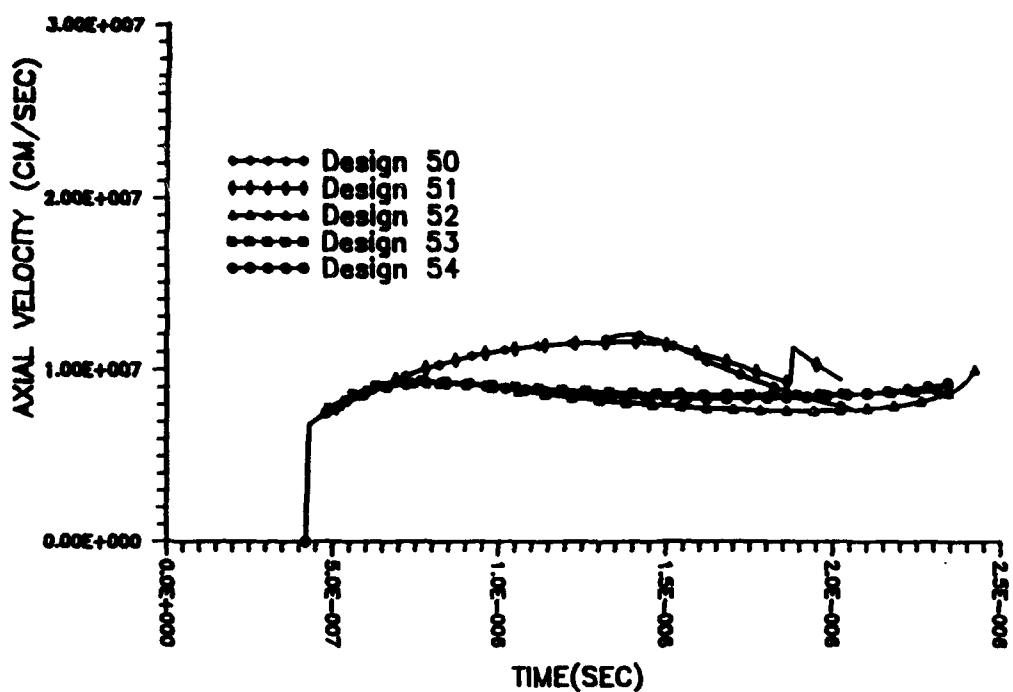
Figure B-7. Graph of Axial Velocity vs. Time for Designs 50-54

42

Appendix C
DPF Circuit Equations and Fortran Program[1]

The circuit equations for the UI DPF are derived from the circuit drawing in Figure C-1. The equations are as follows:

$$(R_e + R_f) I + L_e \frac{dI}{dt} + L_f \frac{dI}{dt} + I \frac{dL_f}{dt} = V_c \qquad \text{(1C)}$$

and

$$\frac{dV_c}{dt} = -\frac{I}{C} \qquad \text{(2C)}$$

where:

R_e = Resistance of the focus assembly

R_f = Resistance of the load (electrodes and the plasma)

I = Current

L_e = Inductance of the focus

L_f = Inductance of the electrodes

V_c = Capacitor voltage

C = Capacitance

The circuit equations for the system are valid for all modes of operation.

The inductance of the focus is calculated from the following equations:

For the lift-off phase:

$$L_{lo} = \frac{\mu_0 Z_0}{2\pi} \ln\left(\frac{R_{sh}}{R_{in}}\right) \qquad \text{(3C)}$$

---

1. Excerpted from: Temple, Brian A. "Design of a Gas Injection System for the Dense Plasma Focus." Masters Thesis, Department of Nuclear Engineering, University of Illinois at Urbana-Champaign, Urbana, IL, 1992.

50Ω

$10nH$ $2nH$ $8nH$

Spark Switch
Inductance   Line Resistance   Line Inductance   Mounting Plate
                       $(R_e + R_f)$ and Gun Inductance

Bank Internals
$24.5nH$

DPF Inductance
(Time Dependent)
L_f

Bank Capacitance
$40\mu f$
$25kV$
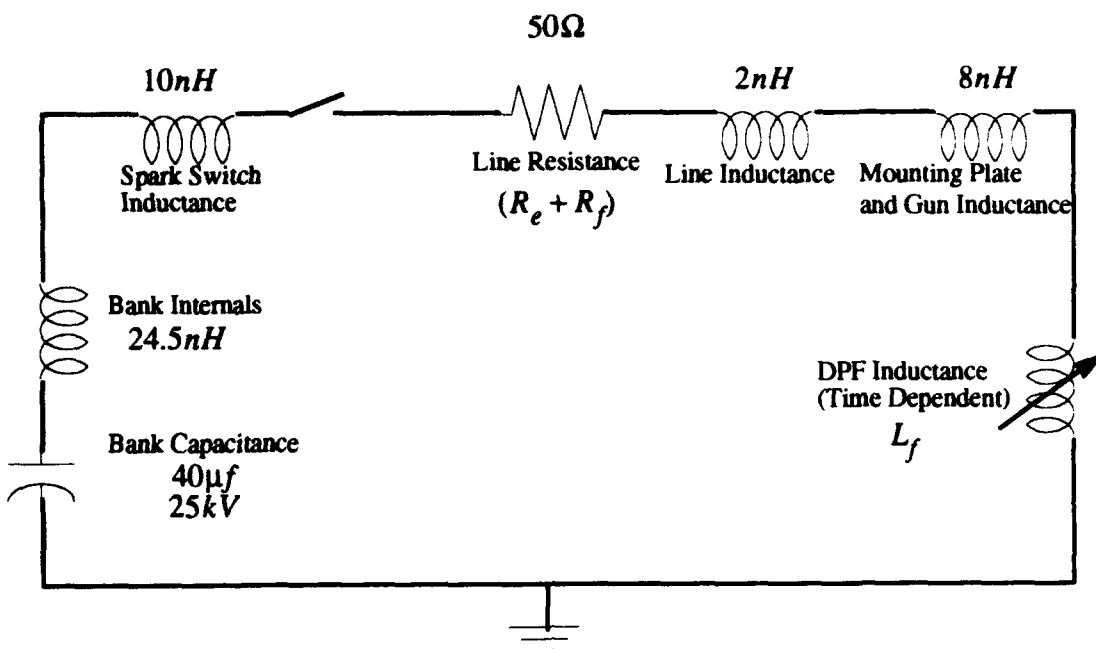
Figure C-1. The DPF Circuit Diagram.

For the rundown phase:

$$L_{rd} = \frac{\mu_0 Z}{2\pi} \ln\left(\frac{R_{out}}{R_{in}}\right)$$ (4C)

Where:

Z_0 = Height of the insulator

R_{sh} = Radius of the sheath

Z = Height of the arc rundown

R_{out} = Radius of the outer electrode

These equations assume that plasma resistance is small compared to the system resistance and dLf/dt is zero. The lift-off inductance is not weighed in the empirical equation for the maximum current and for electrode modifications beyond the height of the insulator. Thus only the rundown inductance is of concern.

The circuit equation is coupled to the equation of motion for the current sheath. In the rundown phase the acceleration of the current sheath is assumed to be negligible. The

44

pressure balance between the magnetic pressure and the rate of momentum gain per unit area define the equation of motion for the current sheath, given as:

$$\frac{B^2}{2\mu_0} = \rho V^2 \tag{5C}$$

Where:

$$B_\theta = \frac{\mu_0 I}{2\pi R_{sh}} \tag{6C}$$

Equation (5C) holds only for a DPF operated in the static fill mode.

Modifications were made to Mandrekas's code[1] to account for the effects from the change in inner electrode geometry. The code was rewritten with the lift-off and rundown calculations being performed in the subroutines LIFT and RUNDOWN instead of being solved in the main body of the code. However, the circuit equation is still solved by a fourth order Runge-Kutta method in the main body of the program. The RUNDOWN subroutine had to be modified to include the effects from the inner electrode radius change. Also an additional subroutine named CRAMER was added to Mandrekas's rundown code to calculate the various electrode geometries desired.

The subroutine CRAMER is used to give a quadratic curve fit to the numbers entered at the start of the program. Initially the program asks for the input of numbers which relate to three points that describe the radial surface of the inner electrode. The values are checked to ensure the numbers given correlate to the correct range of possible values. Subroutine CRAMER sets up a series of three quadratic equations where the radius of the electrode R is the independent variable and the axial position Z is the dependent variable. For a set of three points (R_1, Z_1), (R_2, Z_2), and (R_3, Z_3), the system of equations are:

$$AR_1^2 + BR_1 + C = Z_1 \tag{7C}$$

$$AR_2^2 + BR_2 + C = Z_2 \tag{8C}$$

$$AR_3^2 + BR_3 + C = Z_3 \tag{9C}$$

The unknowns in the three equations are the polynomial coefficients A, B, and C which must be the same in each equation. By using Cramer's rule on the system of linear

---

1. Mandrekas, John. "Zero-Dimensional Model for the Dense Plasma Focus." Masters Thesis, Department of Nuclear Engineering, University of Illinois at Urbana-Champaign, Urbana, IL, 1984.

45

equations for A, B, and C each polynomial coefficient can be found. The general quadratic equation which results, Equation (8C), will give the correct axial distance for each radial value entered into the equation.

$$AR^2 + BR + C = Z \tag{10C}$$

Subroutine LIFT describes the lift-off phase of the arc formation and rundown. Once the current reaches a critical value the current sheath will expand radially outward to the outer electrode radius. This subroutine uses the equation of motion given by Equation (3C) to calculate the radial velocity. The change in radial position for the time increment is then found and added to the prior radial position. Inductance and inductance per unit time can then be calculated and passed back for use in the circuit equation.

Once the current sheath radially expands out to the outer electrode radius the RUNDOWN subroutine is used to model the arc movement. To account for the change in electrode radius the quadratic equation generated from subroutine CRAMER, Equation (8C), is rewritten in the form of:

$$R = -\frac{B}{2} \pm \left(\frac{B^2}{4} - A\,(C - Z) \right)^{\frac{1}{2}} \tag{11C}$$

If-then statements are used to determine which radial value is the correct one for the electrode. Once this is found, the computed radial value is used as input to calculate the axial velocity, inductance per unit length, and the inductance per unit time.

The previous version of the code utilized Equations (5C) and (6C) in the rundown to calculate inductance and inductance per unit length. In Equations (5C) and (6C) the inductance is independent of the step size of the axial rundown. Thus they are only valid for electrodes of constant radius since any change in the radius changes the radius of the entire electrode length. To account for radius changes in a stepwise manner, Equation (6C) was rewritten as:

$$L_{rd\,(n+1)} = L_{rd\,(n)} + \frac{\mu_0}{2\pi}\,(V_Z)\,H\,\,Ln\left(\frac{R_{out}}{R_{in}}\right) \tag{12C}$$

46

Where:

$L_{rd\,(n)}$ = Inductance of previous rundown step

V_Z = Axial velocity

H = Time increment.

Equation (10C) maintains a constant radius for only the length of the axial rundown step size. Accuracy of the equation is limited by the time increment H and the axial velocity V_Z which is calculated from Equation (3C). Greater accuracy can be achieved by decreasing the time increment. The radius of the current sheath (RPR) had to be modified to include the additional arc length from the change in radius. This was performed by adding Equations (11C) and (12C) which find the change in radius and add it to the current length (RPR).

$$\Delta R_{(n+1)} = 2.54 - R_{in\,(n+1)} \tag{13C}$$

$$\Delta RE_{(n+1)} = \Delta RE_{(n)} + \Delta R_{(n+1)} \tag{14C}$$

Where:

$\Delta R_{in\,(n+1)}$ = Radius of the inner electrode at this increment

$\Delta R_{(n+1)}$ = Change in arc length

$\Delta RE_{(n)}$ = Distance between electrodes (arc length) at given increment

$\Delta RE_{(n+1)}$ = (RPR) Radius between electrodes.

The axial velocity, axial position, inductance, arc length, and inductance per unit time are passed on to the main program where they are used in the circuit equation and other calculations.

The program structure of the main body consists of dividing the formation of the arc and the rundown into two parts. Initial conditions and parameters are set at the beginning and values for the electrode surface are entered. Subroutine LIFT is called by the main loop while the current sheath is forming and is radially expanding to the outer electrode radius. Once the arc length reaches the outer electrode radius the program calls up subroutine RUNDOWN which models the rundown of the arc between the electrodes. Each subroutine has no internal loops and the values of the inductance and inductance per unit length calculated in the subroutines are used as input for the circuit equation. The circuit equation for the system is solved by a fourth order Runge-Kutta method. Toward the end of the program the time step is advanced and different circuit values are written in a file. The program terminates once the arc rundown reaches the end of the inner electrode.

The programs are shown on the following pages.

47

```
CC          ZERO4.FOR FORTRAN PROGRAM
CC    THIS PROGRAM CALCULATES THE LIFT-OFF AND RUNDOWN
CC      PHASES OF THE PLASMA FOCUS DISCHARGE, USING
CC                          P.ELTGROTH'S MODEL
CC    ZERO4 VARIES THE INNER ELECTRODE GEOMETRIES

CC    IPL: PLASMA CURRENT
CC    VC : CAPACITOR VOLTAGE
CC    LPF: SELF-INDUNCTANCE OF FOCUS
CC    LPFDL: INDUCTANCE/UNIT LENGTH
CC    C  : CAPACITANCE
CC    LO : EXTERNAL INDUCTANCE
CC    VR : RADIALLY VELOCITY (LIFT-OFF)
CC    VZ : AXIAL VELOCITY (RUNDOWN)
CC     Z : AXIAL DISTANCE TRAVELED BY PLASMA
CC    VPL: VOLTAGE OF PLASMA
CC    IDOT: CURRENT OF SHEATH
CC    NUM: NUMBER OF ITERATIONS(NANOSECONDS)


      REAL IPL,VC,LPF,LO,ILO,DLDT,LS,IDOT,VR,VZ,Z,ROUT
      REAL RIN,H,ZINJ,PR,TIME,CO,PO,VPL,REND,ZTAP,RMID
      REAL A,B,C,ZMID,LPFDL,DELR,RPR
      INTEGER FLAG,NUM

      COMMON RIN,ZTL,ZLO,IPL,ILO,PI,PO,H
      COMMON REND,ZTAP,ROUT,RMID,ZMID


      F1(IPL,VC)=(VC-IPL*(R+DLDT))/(LO+LPF)
      F2(IPL)=-IPL/CO

CC    UNITS FOR CALCULATIONS ARE AS FOLLOWS
CC    VOLTAGES ------------- VOLTS
CC    CURRENT ------------- AMPS
CC    CAPACITANCE ---------- FARADS
CC    RESISTANCE ----------- OHMS
CC    INDUCTANCE ----------- HENRIES
CC    RADIAL DISTANCES ----- CM
CC    AXIAL DISTANCES ------ CM
CC    TIME ----------------- SECONDS
CC    VELOCITES ------------ CM/SEC

      OPEN (UNIT=26,FILE=' NOUTC4.DAT')
      NUM=10000
      PR=6
      VC=25000
5     PRINT*,'ENTER AXIAL DISTANCE OF MODIFICATION IN CM'
      READ(*,*)ZTAP
10    PRINT*,'ENTER END RADIUS OF INNER ELECTRODE IN CM'
```

48

```fortran
        READ(*,*)REND
15      PRINT*,'ENTER MIDPOINT AXIAL DISTANCE IN CM'
        READ(*,*)ZMID
20      PRINT*,'ENTER MIDPOINT RADIAL DISTANCE IN CM'
        READ(*,*)RMID

        CO=40.E-6
        R=3.5E-3
        LO=24.50E-9
        LS=45.E-9
CC      PO IS THE FILL DENSITY COMPUTED FROM THE PRESSURE
        PO=(PR*2*(1.33E+2)*1.0E-6/(8.314*295))
        PI=.31415927E+1
        ILO=35.E+3
CC      GEOMETRIC DIMENSIONS (CM)
        RIN=.254E+1
        ROUT=.5E+1
        R11=.42E+1
        ZLO=.32E+1
        ZTL=1.96E+1

        IF(ZTAP.GT.ZTL.OR.ZTAP.LT.ZLO)THEN
            PRINT*,'ENTER NEW AXIAL MOD. POINT'
            GO TO 5
        ENDIF
        IF(REND.GT.RIN.OR.REND.LT.0.0)THEN
            PRINT*,'ENTER NEW RADIUS ENDPOINT'
            GO TO 10
        ENDIF
        IF(ZMID.GT.ZTL.OR.ZMID.LT.ZLO)THEN
            PRINT*,'ENTER NEW AXIAL MIDPOINT'
            GO TO 15
        ENDIF
        IF(RMID.GT.RIN.OR.RMID.LT.REND)THEN
            PRINT*,'ENTER NEW RADIUS MIDPOINT'
            GO TO 20
        ENDIF

        WRITE(26,100) RIN,ZTAP,RMID,ZMID,REND,ZTL
100     FORMAT(1X,'POINTS',1X,3('(',F6.2,',',F6.2,')',2X))

CC      INITIAL CONDITIONS
            IPL=0.0E+1
            TIME=0.0E+1
            H=1.E-9
            RPR=R11
            Z=ZLO
            FLAG=1
            VR=0.0E+1
```

```fortran
          VZ=0.0E+1
          LPF=2.E-9*ZLO*ALOG(RPR/RIN)
          LPFDL=2.E-9*ALOG(RPR/RIN)
          DLDT=0.0E+1
          VPL=VC-F1(IPL,VC)*13.E-9
          IDOT=F1(IPL,VC)
      CALL CRAMER(A,B,C,REND,RMID,RIN,ZTL,ZMID,ZTAP)
      WRITE(26,120) A,B,C
120   FORMAT(1X,'A=',E12.5,3X,'B=',E12.5,3X,'C=',E12.5)
          WRITE(26,180) TIME,IPL,VPL,LPFDL,VZ,Z,VC,LPF


          DO 1000 J=1,NUM
          IF(RPR.LT.ROUT)THEN
              CALL LIFT(VR,RPR,LPF,DLDT,IPL,ILO,PI,PO,H,RIN,ZLO,LPFDL)
              GO TO 45
          ELSE
              CALL
                  RUN(RIN,Z,VZ,LPF,DLDT,REND,RPR.ZTAP,IPL,ILO,PO,A,B,C,L
                  PFDL)
              GO TO 45
          ENDIF

45        P1=H*F1(IPL,VC)
          P2=H*F2(IPL)
          Q1=H*F1(IPL+P1/2.,VC+P2/2.)
          Q2=H*F2(IPL+P1/2.)
          R1=H*F1(IPL+Q1/2.,VC+Q2/2.)
          R2=H*F2(IPL+Q1/2.)
          S1=H*F1(IPL+R1,VC+R2)
          S2=H*F2(IPL+R1)
          IPL=IPL+(P1+2.*Q1+2.*R1+S1)/6.
          VC=VC+(P2+2.*Q2+2.*R2+S2)/6.
          VPL=VC-F1(IPL,VC)*13.E-9
          IDOT=F1(IPL,VC)
          TIME=TIME+H
          IF(MOD(J,10).EQ.0) THEN
50            WRITE(26,180) TIME,IPL.VPL,LPFDL,VZ,Z,VC,LPF
          IF(Z.GT.ZTL) GO TO 200
          ENDIF
1000      CONTINUE
180   FORMAT(1X,8(E12.5,1X))
200   CLOSE(26)
      END


      SUBROUTINE CRAMER(A,B,C,REND,RMID,RIN,ZTL,ZMID,ZTAP)
      REAL REND,ZTAP,RMID,ZMID,RIN,A,B,C,ZTL,ZLO
      REAL A11,A12,A13,B11,B12,B13,C11,C12,C13,D1,D2,D3
      REAL ANS1,ANS2,ANS3,DETERM,NUMA1,NUMA2,NUMA3,NUMA
```

```
REAL NUMB1,NUMB2,NUMB3,NUMB,NUMC1,NUMC2,NUMC3,NUMC

A11=REND**2
A12=REND
A13=1.0

B11=RMID**2
B12=RMID
B13=1.0

C11=RIN**2
C12=RIN
C13=1.0

D1=ZTL
D2=ZMID
D3=ZTAP

ANS1=A11*((B12*C13)-(C12*B13))
ANS2=-B11*((A12*C13)-(A13*C12))
ANS3=C11*((A12*B13)-(A13*B12))
DETERM=ANS1+ANS2+ANS3

NUMA1=D1*(B12*C13-C12*B13)
NUMA2=-D2*(A12*C13-A13*C12)
NUMA3=D3*(A12*B13-A13*B12)

NUMA=NUMA1+NUMA2+NUMA3

NUMB1=-D1*(B11*C13-C11*B13)
NUMB2=D2*(A11*C13-A13*C11)
NUMB3=-D3*(A11*B13-A13*B11)

NUMB=NUMB1+NUMB2+NUMB3

NUMC1=D1*(B11*C12-C11*B12)
NUMC2=-D2*(A11*C12-A12*C11)
NUMC3=D3*(A11*B12-A12*B11)

NUMC=NUMC1+NUMC2+NUMC3

A=NUMA/DETERM
B=NUMB/DETERM
C=NUMC/DETERM
RETURN
END


SUBROUTINE LIFT(VR,RPR,LPF,DLDT,IPL,ILO,PI,PO,H,RIN,ZLO,LPFDL)
REAL VR,RPR,LPF,DLDT,IPL,ILO,PI,PO,H,RIN,ZLO,LPFDL
```

```
                IF(IPL.LE.ILO) THEN
                    VR=0.0E+1
                    GO TO 30
                ELSE
                    VR=((IPL*IPL-ILO*ILO)/(200.*PI*PO))**(.5)/RPR
                ENDIF
30              RPR=RPR+VR*H
                LPF=2.E-9*ZLO*ALOG(RPR/RIN)
                LPFDL=2.E-9*ALOG(RPR/RIN)
                DLDT=2.E-9*ZLO*VR/RPR
            RETURN
            END


        SUBROUTINE
RUN(RIN,Z,VZ,LPF,DLDT,REND,RPR,ZTAP,IPL,ILO,PO,A,B,C,
    /LPFDL)
        REAL RIN,Z,VZ,LPF,DLDT,A,B,C,VAL,RINA,RINB,LPFDL
        REAL REND,ZTAP,IPL,ILO,PI,PO,H,ROUT,RENDX,RINX
        REAL RPR,DELR
        RENDX=REND-.05
        RINX=RIN+.05
        ROUT=.5E+1
        ZTL=1.96E+1
        H=1.0E-9
        PI=.31415927E+1
        IF(Z.LT.ZTAP)THEN
            GO TO 40
        ELSE
            VAL=(B*B-4.0*A*(C-Z))
            IF(VAL.LT.0.0)THEN
                PRINT*,'ERROR IN POINT VALUES'
                STOP
        ENDIF
        RINA=(-B+SQRT(VAL))/(2*A)
        RINB=(-B-SQRT(VAL))/(2*A)
        IF(RINA.GT.RENDX.AND.RINA.LT.RINX)THEN
            RIN=RINA
            GO TO 40
        ENDIF
        IF(RINB.GT.RENDX.AND.RINB.LT.RINX)THEN
            RIN=RINB
            GO TO 40
        ENDIF
            PRINT*,'   '
            PRINT*,'INCORRECT POINT VALUES'
            PRINT*,RINA,'  ',RINB
        ENDIF
40      VZ=((IPL*IPL-ILO*ILO)/(200.*PI*PO))**(.5)/RIN
```

```
            Z=Z+H*(VZ)
            DELR=(2.54-RIN)
            RPR=RPR+DELR
            LPFDL=2.E-9*ALOG(RPR/RIN)
            LPF=LPF+LPFDL*H*(VZ)
            DLDT=2.E-9*VZ*ALOG(RPR/RIN)
RETURN
END
```

Appendix D
DPF Timing Circuit Program[1]

The NU2.FOR FORTRAN program is one of several programs developed to run the timing circuit for the DPF. Each program runs different peripheral devices. All programs are of the same format and control the opening of the ring valve and the firing of the Marx generator.

Communication between the computer and the relay circuits is carried out by the BITINS and BITOUS subroutines in the programs. These subroutines are previously developed programs used for other experiments. The compiled execution files for these subroutines were linked to the execution file for NU2.FOR during compilation and link editing.

The DELAY subroutine used in the program is another previously developed program that was used as a timing program in other experiments. This subroutine delays the trigger signal to the relevant relay circuit so that the relay circuit can be triggered at the desired time. Thus each peripheral device can operate at the proper time in the sequence.

Input for the program is stored in the file named TIMEDATA.DOC.

---

1. Excerpted from: Temple, Brian A. "Design of a Gas Injection System for the Dense Plasma Focus." Masters Thesis, Department of Nuclear Engineering, University of Illinois at Urbana-Champaign, Urbana, IL, 1992.

```fortran
c NU2.FOR
c Program to control the firing sequence for Plasma Focus
c Experiments with axial B-field control
c
c Uses the IBM DACA board
c
c
      integer*2 adapt,device,bits,bitv,bitf,rawval,
     * bita,bitb,bitc,stat,stats,statt
      integer*4 ovhd,fd,rfd,frv,d,d1,d2,d3
      character*1 ans,start
      character*6 name1,name2,name3
c
      adapt=0
      device=8
      ovhd = 20
c BIT 11 IS FOR THE MARX GEN.
      bitf=11
c BIT 12 IS FOR THE SOLENOIDS
      bita=12
c BIT 13 IS FOR THE AXIAL B-FIELD
      bitb=13
      rawval=1
      stat=0
c TURN ON SOLENOID RELAY
      call bitous(adapt,device,bitf,rawval,stat)
      if(stat.ne.0) then
          write(*,50) bitf
      endif
      call bitous(adapt,device,bita,rawval,stat)
      if(stat.ne.0) then
          write(*,50) bita
50        format(1x,'Execution error on bit',i3)
          goto 1000
      endif
      call bitous(adapt,device,bitb,rawval,stat)
      if(stat.ne.0) then
          write(*,50) bitb
          goto 1000
      endif
c
c LOAD INPUT PARAMETERS
c
100   open(7, file='timedata2.doc', status='old')
      read(7,105)name1,fd,name2,frv,name3,rfd
105   format(a6,i4,a6,i4,a6,i4)
      close(7, status='keep')
c
c formerly GOSUB 10000
c Safety Interlock
```

```
c bit input 15 is solenoid
c bit input 14 is vacuum valve
        bits = 15
        bitv = 14
        stat=0
        rawval=1
        call bitins(adapt,device,bits,rawval,stat)
        if (stat.ne.0) goto 200
        if (rawval.eq.0) goto 122
        stat=0
        rawval=1
        call bitins(adapt,device,bitv,rawval,stat)
        if (stat.ne.0) goto 200
        if (rawval.eq.0) goto 112
c
        write(*,*)'  '
        write(*,*)'Solenoids are OFF.'
        write(*,*)'Vacuum Valve is CLOSED.'
        go to 400
c
 112    write(*,*)'ERROR! - Vacuum Valve is OPEN.'
        goto 1000
c
 122    write(*,*)'ERROR! - Solenoids are ON.'
        goto 1000
c
 200    write(*,204) stat
 204    format(1x,'Execution Error ',i6)
        goto 1000
c
c formerly GOSUB 1000
 400    write(*,*)'  '
        write(*,410) fd
 410    format(1x,'The present FD value is ',I4,' ms')
        write(*,420) frv
 420    format(1x,'The present FRV value is ',i4,' ms')
        write(*,*)'  '
        write(*,*)'Do you want to set the time intervals for'
        write(*,*)'the Firing Delay Time (FD)and the Ring'
        write(*,*)'Valve Closing time (FRV)'
        write(*,*)'  '
        write(*,*)'Enter Y=Yes or N=No:'
        read(*,'(a)') ans
        if(ans.eq.'N') goto 500
        if(ans.eq.'n') go to 500
        if(ans.eq.'Y') go to 450
        if(ans.eq.'y') go to 450
        go to 900
c
c SET FIRE DELAY TIME AND RING VALVE CLOSING TIME
```

```
c
 450   write(*,*)' '
       write(*,*)'Enter the Fire Delay Time in milliseconds'
       read(*,'(i4)') fd
       write(*,*)'Enter the Ring Valve Closing Time in'
       write(*,*)'milliseconds'
       read(*,'(i4)') frv
c

 500   write(*,*)'  '
       write(*,510) rfd
 510  format(1x,'The present RFD value is: 'i4,' ms')
       write(*,*)'  '
       write(*,*)'Do you want to change the Ring Valve'
       write(*,*)'Delay time (RFD)'
       write(*,*)'Enter Y=Yes or N=No:'
       read(*,'(a)') ans
       if(ans.eq.'N') goto 600
       if(ans.eq.'n') go to 600
       if(ans.eq.'Y') go to 550
       if(ans.eq.'y') goto 550
       go to 900
c
 550   write(*,*)'  '
       write(*,*)'Input Ring Valve Fire Delay Time'
       write(*,*)'in milliseconds'
       read(*,'(i4)') rfd
c
c PRINT OUT NEW VALUES
c
 600   write(*,*)'  '
       write(*,410) fd
       write(*,420) frv
       write(*,510) rfd
       write(*,*)'  '
       open (7, file='timedata2.doc', status='old')
       write(7,105)name1,fd,name2,frv,name3,rfd
       close(7, status='keep')
c
c FIRING SEQUENCE
c
 700   write(*,*)'To reset hit any key and hit return OR'
       write(*,*)'Hit Return to start firing sequence'
       read(*,'(a)') start
       if(start.ne.' ') goto 1000
       if(start.ne.' ') go to 1000
       write(*,*)'FIRING'
       stat=0
       d=fd-ovhd
c TIME DELAY FOR FIRING
```

```fortran
      call delay(adapt,d,stat)
      if(stat.ne.0) then
          write(*,*)'Status error in firing delay'
          goto 1000
      endif
c TURN ON B-FIELD
      rawval=0
      stat=0
      call bitous(adapt,device,bitb,rawval,stat)
      d3=2000
      call delay(adapt,d3,stat)
      if(stat.ne.0) then
          write(*,*)'Status error in B-field'
          goto 1000
      endif
c TURN ON SOLENOID RELAY
      rawval=0
      stat=0
      call bitous(adapt,device,bita,rawval,stat)
      stats=0
      statt=0
c SET TIME INTERVALS
      rawval=0
      d1=rfd-ovhd
      d2=frv-ovhd
c TIME DELAY FOR FIRING MARX GEN.
      call delay(adapt,d1,stats)
      if(stats.ne.0) then
          write(*,*)'Status error in ring valve delay'
          goto 1000
      endif
c OPEN GAS VALVE MARX GENERATOR
      call bitous(adapt,device,bitf,rawval,stats)
      if(stats.ne.0) then
          write(*,50) bitf
          goto 1000
      endif
c TIME DELAY FOR CLOSING OF SOLENOIDS
      call delay(adapt,d2,stats)
c TURN OFF SOLENOIDS AND B-FIELD
      rawval=1
      stat=0
      write(*,*)'Execution complete'
      call bitous(adapt,device,bita,rawval,stat)
      call bitous(adapt,device,bitb,rawval,stat)
c
c CLOSE MARX GEN. GAS VALVE
      rawval=1
      stats=0
      call bitous(adapt,device,bitf,rawval,stats)
```

```fortran
      go to 1000
c
c END OF PROGRAM
c
 900  write(*,*)'ERROR IN INPUT'
      write(*,*)'   '
1000  write(*,*)'Do you want to Pulse again'
      write(*,*)'Enter Y=Yes or N=No:'
      read(*,'(a)') ans
      if(ans.eq.'Y') go to 100
      if(ans.eq.'y') go to 100
9999  end
```